Russian Chemical Reviews **74** (3) 265 – 283 (2005) © 2005 Russian Academy of Sciences and Turpion Ltd

DOI 10.1070/RC2005v074n03ABEH000876

The shape memory effect in polymers

V A Beloshenko, V N Varyukhin, Yu V Voznyak

Contents

I.	Introduction	265
II.	Glassy polymers	265
III.	Crystallisable polymers	270
IV.	Polymer blends and filled polymer composites	275
V.	Polymer gels	279
VI.	Conclusion	280

Abstract. The review concerns the state-of-the-art in the field of investigations of the shape memory effect in various polymeric materials, namely, homopolymers, copolymers, polymer blends, filled polymer composites and polymer gels. New theoretical approaches to the description and practical applications of the shape memory effect are discussed. The bibliography includes 205 references.

I. Introduction

Many polymers are used as structural materials for the production of various items and equipment.[1–3] Such materials must exhibit certain mechanical properties and operating characteristics and their production must be simple and cost-efficient. Another group of materials comprises the so-called functional polymeric materials. The function and field of application of such materials are mainly determined by the specific and sometimes unique properties they possess. Typical representatives of this class of compounds are polymers and polymer composites that possess the ability to recover their shape.

The 'shape memory effect' (SME) is characteristic of not only polymers. Initially, the term 'SME' was mainly used for metal alloys. In the case of high-molecular-mass compounds, the term 'thermal shrinkage' was often used because most studies on the problem were concerned with shape recovery features of stretched samples.

In this review we consider the behaviour of polymers deformed in various manners by applying a tensile, compression or shear deformation; therefore, the use of the term 'SME' seems to be appropriate. This effect manifests itself in a complete or partial recovery of the initial size of samples of simple geometrical shape exposed to external action. However, in some cases (if, *e.g.*, the shape variation obeys a 'rod – helix – rod' pattern) it is more appropriate to place the emphasis on the shape.

V A Beloshenko, V N Varyukhin, Yu V Voznyak A A Galkin Donetsk Physics and Technology Institute, National Academy of Sciences of Ukraine, ul. R Luxemburg 72, 83114 Donetsk, Ukraine.
Fax (38-062) 337 90 18, tel. (38-062) 337 93 30,
e-mail: bel@hpress.dipt.donetsk.ua (V A Beloshenko),
tel. (38-062) 255 05 18, e-mail: var@hpress.dipt.donetsk.ua
(V N Varyukhin), tel. (38-062) 334 86 95 (Yu V Voznyak)

Received 12 January 2004
Uspekhi Khimii **74** (3) 285 – 306 (2004); translated by A M Raevskiy

Pioneering communications on the SME in metal alloys and polymers were reported nearly five decades ago. Recently, numerous monographs concerning the SME in metallic materials have been published.[4–10] At the same time there are quite a few monographs or reviews on the shape memory effect in polymers and the results reported are mainly concerned with the behaviour of oriented synthetic fibres.[11–14] A detailed review [15] published in 1992 was also incomprehensive because the authors restricted themselves to coverage of some fundamental problems of thermal shrinkage of oriented homopolymers. That review included no data on more complex polymer systems and contained little information on applied studies and almost no information on investigations carried out by Russian researchers.

Since then there has been a considerable amount of literature on the SME in polymers. The subjects were the development of theoretical concepts of the mechanisms of thermally stimulated strain recovery; new approaches to the description of the deformation and relaxation behaviour of polymers; new information on the shape recovery features of deformed samples; and results of investigations of synthetic polymeric materials possessing unusual properties. Because research in the field covers a wide variety of aspects of the title problem, here we first of all tried to highlight the key recent advances and provide information on modern investigaton avenues and practical applications of the SME.

According to Irie,[16] the SME in polymeric materials can be realised in three ways. The first way involves the formation of a shaped sample from melt. If necessary, cross-links can be formed by adding cross-linking agents or by irradiating the sample. Then, the sample is deformed at a temperature similar to the glass transition temperature, T_g, or the melting point, T_m, and cooled in order to retain the deformed state. Shape recovery is attained by heating the sample above T_g or to T_m. The second way involves a photochemically or electrochemically induced reversible change in the shape of the polymer sample. The third way involves a shape change induced by chemical reactions. In the objects considered in this review the SME occurs following the first way, *i.e.*, on heating. The mechanism and specific features of this kind of SME are to a great extent determined by the nature (structure and morphology) of the polymer.

II. Glassy polymers

Shape recovery of deformed polymers originates from the system's 'quest' for thermodynamic equilibrium, which is determined by the minimum value of the corresponding thermodynamic potential (*i.e.*, the difference between the internal energy and the

entropy of the components of the macromolecules in the polymer system). Strain-induced orientation of polymer chains causes the entropy of the system to decrease. Therefore, shape stability of a strained polymer would depend on the change in the internal energy. If the internal energy decreases on deformation and compensates the decrease in entropy, a stable structure is formed. This situation can be realised in crystallisable polymers where bonding between polymer chains is strong enough. In glassy polymers, the strain-induced nonequilibrium state is retained only after cooling below T_g. Because these differences to a great extent determine the laws of manifestation of the SME in the materials mentioned above, they deserve a separate consideration.

Without dwelling on details of macroscopic manifestation of the SME in glassy polymers (most of them have been reviewed [15]), we will point out the most characteristic features. Oriented glassy polymer samples (at least those having a simple shape) completely recover their initial size after heating to the glass transition temperature. The process begins at $T < T_g$ and its rate and degree of shape recovery increase as the temperature increases.

By fixing the ends of a deformed sample and measuring mechanical stress developed during the constrained recovery it is possible to study the early stages of recovery, characterised by small variation of the size. Typical temperature dependences of shrinkage stress for polycarbonate (PC) oriented by stretching at room temperature with heaing at a constant rate are shown in Fig. 1. For an unannealed PC sample, the shrinkage stress σ_s begins to increase at a temperature that is slightly higher than the stretching temperature, reaches a maximum at $T < T_g$ and decreases down to zero as the temperature approaches T_g. Heating of an annealed PC sample to a temperature below the annealing temperature causes the shrinkage to virtually disappear. The position of the maximum in the $\sigma_s(T)$ plot is shifted towards higher temperatures and its height decreases. At the same time the zero σ_s value is achieved under the same conditions as in the case of the unannealed sample, *i.e.*, near T_g.

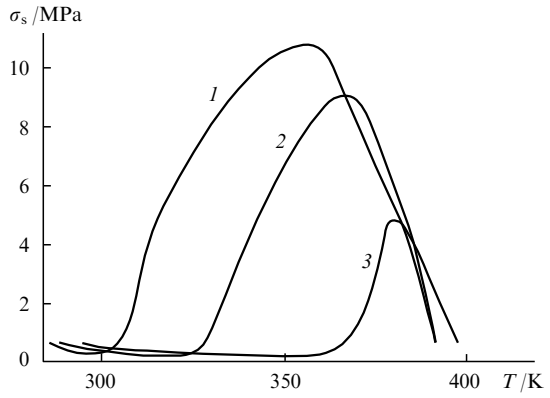


Figure 1. Isometric heating curves for PC.[17]
Unannealed sample (*1*) and samples annealed at 348 (*2*) and 398 K (*3*).

If a sample with fixed ends is kept at a temperature that is higher than the deformation temperature but much lower than T_g, an induction period is observed (Fig. 2).[18] Duration of the induction period depends on the test temperature and sample prehistory and can vary by one or even two orders of magnitude. It is believed [18] that the phenomenon can be explained by a high degree of localisation of thermally stimulated molecular shrinkage in certain regions of the amorphous polymer. Activated molecular segments 'try' to shorten the distances between their ends; however, ambient macromolecules preclude shrinkage. Shrinkage forces developed in activated segments are responsible for compression stress in the vicinity of these segments. Therefore, further thermal activation of macromolecules will most probably be followed by shrinkage in the compressed regions. The higher the

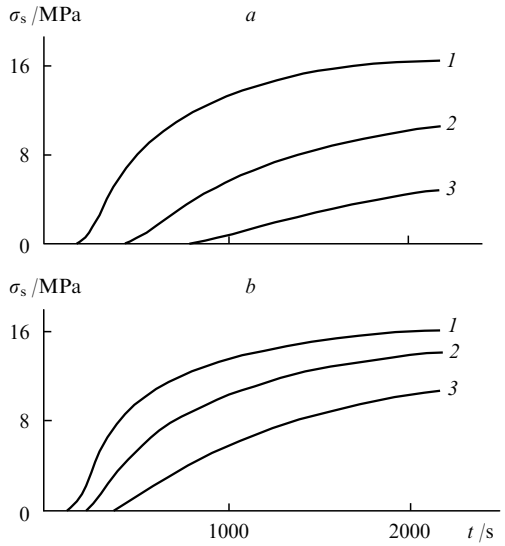


Figure 2. Shrinkage stress plotted *vs*. time for PC.[18]
(*a*) Measured at 323 (*1*), 328 (*2*) and 333 K (*3*) 14 days after deformation; (*b*) measured at 328 K 2 (*1*), 5 (*2*) and 14 days (*3*) after deformation.

degree of thermal activation, the shorter the induction period. At the same time if the activation energy is insufficiently high, local stress can relax owing to chain slip and thus lead to a decrease in the local orientation without corresponding spatial changes.

Shape recovery of glassy polymers is usually described using simplified phenomenological models. Some of them were considered in detail in a review.[15] Such models are usually based on the concept of one or more energy barriers separating different states of the condensed system. The barriers are treated as hindrances to mobile fragments in the bulk of glassy polymer. In particular, a model involving two energy states of a polymer segment was proposed.[19, 20] It was assumed [19, 20] that any molecular chain in an oriented polymer comprises submolecules that can be in the compressed (*a*) or stretched (*b*) states separated by an energy barrier. Assuming a constant number of submolecules in the chain, the relative shrinkage of a model macromolecule induced by temperature variation can be related to the population of states. Transitions between the states are described by the following equation

$$\frac{dn}{dt} = (1 - n_b)k_b - n_b k_a \,, \tag{1}$$

where n_b is the population of the state b and k_a and k_b are the rates of transitions to the states a and b, respectively,

$$k_a = A \exp\left(-\frac{\Delta E + M}{RT}\right), \tag{2}$$

$$k_b = A \exp\left(-\frac{\Delta E + \varepsilon - M}{RT}\right). \tag{3}$$

Here A is a constant, ΔE is the activation energy for shrinkage, M is the energy associated with possible application of external stress and ε is the energy difference between the states.

Using Eqn (1), it is possible to calculate the temporal or temperature dependences of the populations of states and thus establish the corresponding dependence of thermal shrinkage of the model sample. The results obtained using the two-state model are in qualitative agreement with experimental data.[21] However, the model also has significant drawbacks, *e.g.*, it can not predict the onset of shrinkage forces at the ends of the sample in the isometric heating experiments, because no interaction between submolecules is assumed.

According to Trznadel and Kryszewski,[15] a comprehensive rheological model of thermal shrinkage of oriented glassy polymers must account for:

— the possibility of relaxation of molecular orientation by thermally activated transitions,

— the possibility of propagation of local changes throughout the sample owing to the presence of an elastic physical network and

— the possibility of relaxation of the local stress as a result of intermolecular slip.

The four-state [17,22] and multi-state [23,24] mechanical models are successfully used for calculating the temporal and temperature dependences and for providing an explanation for the appearance of the induction period. The local relaxation can be best predicted at low temperatures, *i.e.*, in the absence of large structural changes. At the same time these models are too simple to describe the shrinkage process over a wide temperature region.

Yang and Sun [25] proposed a model based on the theory of conformational elasticity of molecular chains,[26–29] which allows a chain conformation distribution to be obtained with realistic information on the molecules. The model was used to analyse the experimental results of the SME studies in amorphous poly(ethylene terephthalate) (PETP).[26,27] A relation was established between the local structure of PETP and the structure of the entire system. The ensemble-averaged fraction of a local conformation is given by [25]

$$\langle X_s(r)\rangle = [Z_s(r)]^{-1} \int_r^{R_{max}} \int_{E_{min}}^{E_{max}} P(R,E) X e^{-E/kT} dR dE, \qquad (4)$$

where X is the fraction of the *trans*-conformation of OCH_2-CH_2O (ethylene glycol residue); $Z_s(r)$ is the partial distribution function of the system that is locally extended by the distance r; $P(R,E)$ is the chain conformation distribution function and R and E are respectively the chain conformation length and energy.

It was established that dependence (4) fits experimental data well. It was shown that the deformation (extension) and shape recovery of cold drawn glassy polymers are different. The extension process involves at least two stages, *viz*., the yield and molecular coil extension. The third stage, slip, can occur if a certain critical point is reached (in the case under study, at elongations greater than a value of 2.3). The shape recovery process involves a stage characterising the dependence of size on the chain conformation. This fact is explained by differences between the strain and shape recovery rates that are responsible for bringing the molecular chain conformations either closer to or farther apart from the state of thermodynamic equilibrium.

The examples given above show that the thermally stimulated strain recovery mechanism underlying the SME in glassy polymers is rather complicated. It involves the relaxation of the segmental orientation and the molecular chain orientation. These processes were studied [30] in order to establish the differences between the relaxation mechanisms of the local and total molecular orientation taking PC stretched at $T > T_g$ as an example. The degree of segmental orientation was estimated by IR dichroism using function

$$f = \frac{(R_0+2)(R-1)}{(R_0-1)(R+2)}, \qquad (5)$$

where R_0 is the dichroic ratio for the perfectly oriented polymer. The degree of the molecular chain extension was determined as follows

$$\lambda = \frac{L_d}{L_s}, \qquad (6)$$

where L_d is the length of the undeformed sample and L_s is the length of the shrunken sample.

It should be noted that conditions necessary for attainment of high segmental orientation are in contrast to those which lead to a high molecular chain extension. In the first case, rapid stretching at temperatures close to the glass transition temperature are needed. In the second case slow stretching and high temperatures are required. With allowance for this, samples deformed at different temperatures and loads were studied.

The relaxation dynamics of segmental orientation and molecular orientation as functions of the deformation temperature T_d and tensile load F can be followed using the data shown in Figs 3 and 4. The temperatures of deformation and subsequent heating

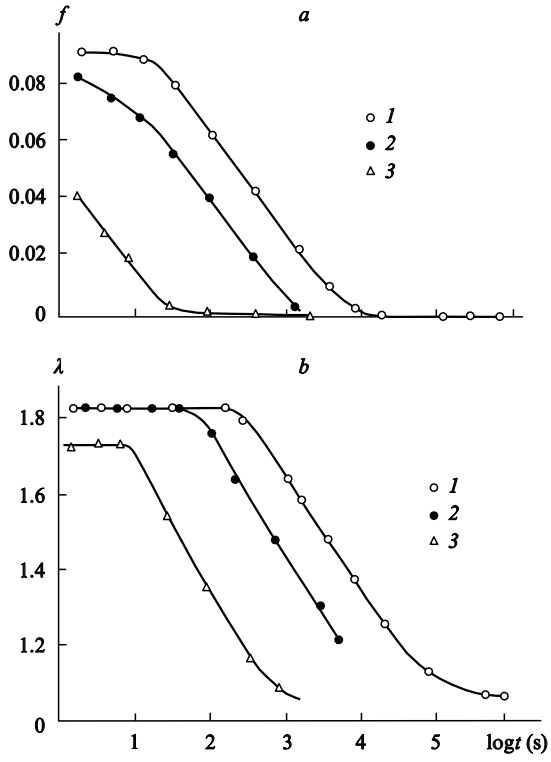


Figure 3. Relaxation of segmental orientation (*a*) and molecular orientation (*b*) in PC plotted *vs*. time at different deformation temperatures.[30] T_d/K: 426 (*1*), 433 (*2*) and 443 (*3*).

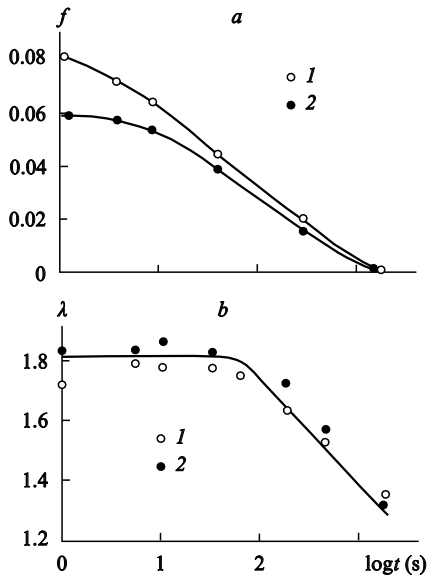


Figure 4. Relaxation of segmental orientation (*a*) and molecular orientation (*b*) in PC plotted *vs*. time at different loads.[30] F/N: 574 (*1*) and 846 (*2*).

were equal. As can be seen, the degree of segmental orientation and the average relaxation time of segmental orientation decrease as the temperature increases (see Fig. 3 *a*). Strain rate (dead load) affects the initial degree of segmental orientation; however, the relaxation time is independent of the strain rate (see Fig. 4 *a*). The character of the relaxation of molecular orientation differs from that described above, namely, an induction period is observed in all $\lambda(\log t)$ plots obtained under the same pre-stretching conditions at all temperatures (see Fig. 3 *b*). The higher the temperature, the shorter the induction period. No effect of the strain rate was observed for the dead load interval studied in this work (see Fig. 4 *b*).

Comparison of the plots constructed in the coordinates $f(\lambda)$ allowed the ratio of the contributions of the segmental orientation and molecular orientation at various heating temperatures and loads to be analysed. It was concluded [30] that in a certain temperature interval an almost total relaxation of segmental orientation can occur without any relaxation of molecular orientation. The samples deformed at a higher rate are characterised by a greater loss of segmental orientation during the time before the start of relaxation of molecular orientation.

The character of the relaxation processes investigated was established based on correlations between f and λ. If the molecular orientation remains unchanged while segmental orientation decreases, the relaxation mechanism is local in character. Its kinetics are independent of the location of the segments along the chain and the process corresponds to a Rouse relaxation between two entanglements.[31] The relaxation of molecular orientation requires large-scale motions which are hindered by surrounding chains. This relaxation corresponds to a contraction inside the tube and to reptation. The results obtained in the study [30] are in good agreement with the assumption [32] that the macromolecule can lose its dichroism owing to local restructuring. They are also consistent with the results obtained by Brown and Windel [33] who found that the molecular orientation is more sensitive to the recovery process than the total deformation.

As a rule, the SME in amorphous polymers occurs without considerable variation of the volume. But if the starting material is characterised by an optimum porosity, shape recovery accompanied by an increase in volume can occur under certain deformation conditions. This is the case in a study [34] where a porous structure was formed in poly(vinyl chloride) (PVC) by dehydrochlorination of PVC powder at 503 K. Compact cylindrical samples of the dehydrochlorinated and cross-linked (in HCl) polymer were then compression deformed in a cylindrical cell of the same diameter. Heating of the samples obtained to $T \geqslant T_g$ was accompanied by uniaxial volume recovery due to elongation of the samples. The effect was most pronounced at a degree of dehydrochlorination, x, of 12.9%.

Structural relaxation was described [34] in the framework of the two-state model. A number of parameters, in particular, the activation energy, population in the equilibrium state and empirical constants, were obtained for various x. Unfortunately, the authors did not discuss microscopic aspects of the SME in the objects under study. Considerable attention was paid to this subject in studies [35, 36] on the mechanism of plastic deformation of glassy polymers. Two stages of shape recovery in polymer glasses were established. These are the low-temperature recovery (LTR) below T_g and the high-temperature recovery (HTR) at T_g. The temperature dependences of the residual strain recovery rates $\dot{\varepsilon}_{res}$ of uniaxially compressed amorphous PETP samples at $T < T_g$ are shown in Fig. 5. Both stages are clearly seen. Analogous dependences were also established for other amorphous polymers.[37, 38] It was shown [35] that the LTR dominates in the early stage of deformation. At high degrees of deformation, the contribution of the HTR to the overall process is much larger than that of the LTR. The contribution of the LTR increases as the deformation temperature decreases; the LTR process always begins near the deformation temperature, whereas the HTR peak lies at T_g.

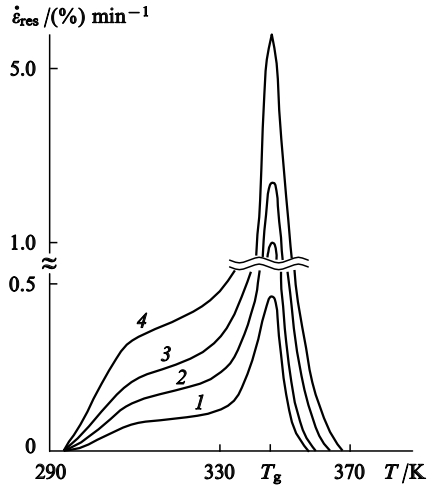


Figure 5. Temperature dependences of the residual strain recovery rates for PETP.[35]
ε_{res} (%): 1.5 (*1*), 4.5 (*2*), 7.5 (*3*) and 14.5 (*4*).

These and other physical processes accompanying deformation of polymer glasses are explained using the concept of shear defects (SD).[35] Each SD bears a local residual shear strain and corresponding local excess internal energy. Similarly to the total excess internal energy, the total macroscopic residual strain of a sample is the sum of all elementary local energies or strains. An elementary act of a deformation process involves initiation and development of an SD. Heating of a deformed sample to $T < T_g$ is accompanied by removal of those SD that are associated with the low-temperature stage of recovery and has no effect on the processes responsible for the HTR. Redeformation of the sample causes no increase in the HTR peak until the fraction of the SD-induced deformation reaches again a certain critical value. In other words, the SD can exist in the absence of the processes that initiate the HTR, but not otherwise. The HTR peaks appear during the annealing (at $T > T_g$) of new conformational structures that were formed in the development of SD. These peaks are always preceded by the appearance of the LTR peaks.

Based on the results of studies on the features of the deformation behaviour of glassy polymers, a concept was proposed,[36] according to which the total inelastic deformation and steady-state plastic flow occur in the polymer structure saturated with small-scale plastic shear transformations (PST) rather than the initial polymer structure. In the former case we deal with an excited and therefore metastable structure and corresponding relaxation processes are closely related to the initiation and loss of PST. The appearance of the LTR peak is due to accumulation of PST, which leads to the total residual strain recovery below T_g. In the plot of the temperature dependence of $\dot{\varepsilon}_{res}$ the area under the LTR peak is a measure of the concentration of the PST that 'survive' in the unloaded (after deformation) polymer at given ε_{res}, T_d and ageing time. An increase in ε_{res} causes an increase in the area under the LTR peak but is not accompanied by any conformational changes in the macromolecular chains. When the PST concentration reaches a critical value, an HTR peak appears in the recovery curves and increases with an increase in degree of strain. The appearance of the HTR peak indicates conformational transformations within distorted chains. At high strain, the HTR peak dominates while the LTR peak is of low intensity; because of this, no LTR stage was detected in the early studies of the SME in amorphous polymers.

The approach of Perez *et al.*[39–41] to the description of deformation of polymer glasses is analogous to that used in the studies mentioned above.[35, 36] According to the model proposed, the main mechanism of deformation in amorphous polymers involves nucleation of localised shear microdomains (SMD) that

carry inelastic strain. The reason for the appearance of plastic deformation is the interaction between two or more SMD, which causes molecular rearrangements and conformational changes in the polymer. Different natures of coupled molecular motions are responsible for different time scales of the recovery of two strain components, namely, inelastic strain and plastic strain (original terms are given) at temperatures $T < (T_g - 20\ \text{K})$.[42,43] The former is characterised by fast relaxation while a slow relaxation is a feature of the latter. Inelastic strain can be completely recovered on heating of the material to $T_g - 20$ K, whereas complete recovery of plastic strain requires heating to at least T_g.[42–44]

The approach[35,36] treats the LTR as a nonequilibrium polychromatic relaxation. In studies[45–49] the low-temperature component of the relaxation of deformed glassy polymers was associated with conformational changes of macromolecular fragments within local structural regions. Taking poly(methyl methacrylate) (PMMA) as an example,[45] it was shown that the LTR of the samples compressed to different deformation values ε at $T < T_g$ can be described by a generalised curve plotted in the coordinates $(\varepsilon - \varepsilon_T) - T$ (Fig. 6 *a*), where ε_T is the residual strain at a given temperature. Analysis of the plots shown in Fig. 6 *a* showed that the sample contains regions characterised by various packing density and local glass transition temperatures. This confirms structural heterogeneity of organic glasses.[50] Loading of material is accompanied by successive involvement of such structural regions in the deformation process and, therefore, in the recovery process on subsequent thermal activation.

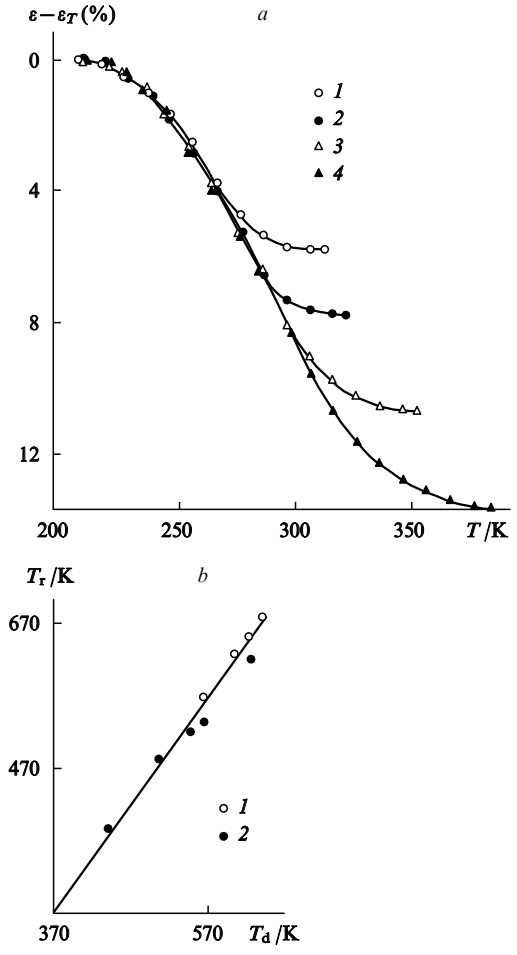


Figure 6. Temperature dependences of the differences $\varepsilon - \varepsilon_T$ (*a*) and the dependence of the total strain recovery temperature on the deformation temperature (*b*) for PMMA samples.[45,48]
(*a*): ε = 6 (*1*), 8 (*2*), 11 (*3*), 14% (*4*); (*b*): uniaxially compressed (*1*) and hydrostatically pressed (*2*) samples.

Treatment of experimental data on thermally stimulated recovery of a large number of deformed polymer glasses allows common features of deformation and recovery of this class of polymers to be established.[46] In particular, the temperature dependences of the residual strain plotted in the coordinates $(\varepsilon - \varepsilon_T)/\varepsilon_{f.e} - (T - T_g)(T_g - T_d)$, where $\varepsilon_{f.e}$ is the strain corresponding to the forced elasticity limit, fall on the same generalised curve as for glassy polymers. This points to a common deformation and subsequent recovery mechanism of glassy polymers, which is due to similarity in their structural organisation. Recovery of deformed polymers is reduced to successive devitrification of the structural regions with different packing densities and local glass transition temperatures.

Taking into account a quasi-equilibrium character of thermally stimulated recovery of deformed glassy polymers at $T < T_g$ (see Ref. 45) and the fact that it can be described by a common generalised curve,[46] it is possible to explain the results,[48] namely, an increase in the complete recovery temperature, T_r, with an increase in the deformation temperature. Indeed, at a specified degree of deformation an increase in T_d is accompanied by involvement of structural regions with higher packing density (within these regions the recovery occurs at higher temperatures) in the deformation process.

Figure 6 *b* presents the complete recovery temperatures of uniaxially compressed (by 6%) and hydrostatically pressed (0.3 GPa) PMMA samples plotted *vs.* deformation temperature.[48] They fall on the same straight line whose extrapolation to $T_r = 0$ K gives a deformation temperature of 100 K. The case $T_r = 0$ means that a PMMA sample deformed at $T_d \leqslant 100$ K undergoes elastic recovery at any temperature, on unloading. With allowance for this fact the temperature found (100 K) can be treated as the transition temperature from ideal elastic deformation to plastic deformation, *i.e.*, the temperature of transition from the brittle failure to the ductile failure mechanism.

Glassy polymers are structurally inhomogeneous. The inhomogeneity size varies from a few to tens of Ångström;[51,52] inhomogeneities have a fluctuative character. This is responsible for severe experimental difficulties in the studies of structural rearrangements, because they can not be visualised by traditional structural methods. Using an original microscopic technique which allows structural rearrangements in deformed amorphous polymers to be visualised, previously unknown features of the LTR were revealed[53,54] and a new mechanism of thermally stimulated recovery of polymer glasses was proposed. The method involves investigation of the structural-mechanical characteristics of deformed polymer films with thin solid coatings.[53–59] A direct microscopic investigation of the structural evolution of the coating during film recovery showed that thermal shrinkage causes the appearance of a regular microrelief on the polymer surface. The character of the microrelief depends only slightly on both the coating material and the substrate material. The relief is characterised by three types of morphological features.[58] The most pronounced is the first type, namely, irregular closed cellular structures formed by rather high buckles of the coating. The second type is represented by specific wavy structures inside the cells with somewhat lower buckles and the third type are rectilinear folds crossing the whole sample. Studies of such a microrelief gave important information on the structural rearrangements accompanying deformation of the polymeric substrate. This information also allows fine details of the LTR to be established.

Characteristic temperature dependences of the size recovery of glassy polymer (PETP) samples deformed below and above T_g are shown in Fig. 7.[54] Planar orientation of the PETP films was performed according to Refs 53 and 60. As can be seen, the size recovery of a film oriented at 373 K mainly occurs near the glass transition temperature. PETP deformed at room temperature completely recovered its size at temperatures below T_g. The LTR during annealing of the PC and PMMA samples deformed

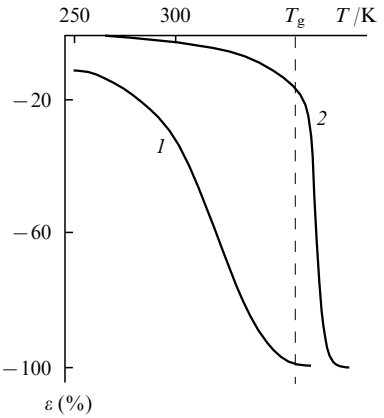


Figure 7. Temperature dependences of strain recovery for PETP.[54]
T_d /K: 293 (*1*) and 373 (*2*).

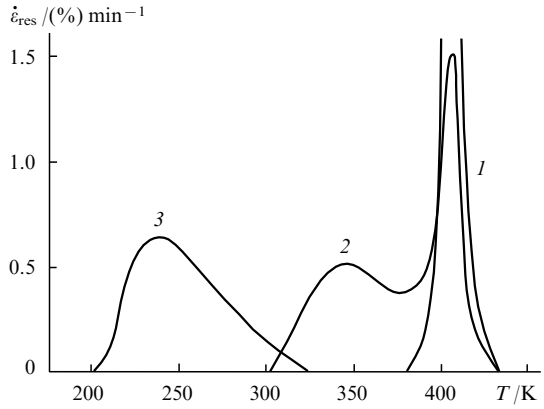


Figure 8. Temperature dependences of residual strain recovery rate for EP.[36]
T_d /K: 423 (*1*), 293 (*2*) and 173 (*3*).

by the classical crazing mechanism[61,62] or by stretching in air occurs analogously.

Deformation of a polymer sample below T_g causes the appearance of specific zones containing oriented polymer and separated by well-defined interfaces.[54,62] In the case of both crazing and the development of shear bands, these zones penetrate thoroughout the bulk of the polymer and impart to the polymer the properties characteristic of oriented highly disperse material. The key factor responsible for the LTR is a decrease in the glass transition temperature of the surface layers. On progressive devitrification of the oriented material, filling the zones of localised deformation induces the force responsible for the LTR. It should be emphasised that the low-temperature recovery occurs in the shear bands that appear during deformation below and near the yield point and retain their individual features even after transition of the whole polymer to the oriented state. That is why the low-temperature shrinkage begins within these zones. The HTR is associated with the relaxation of molecular orientation in the bulk of the polymer, acquired during deformation after the yield point was achieved.[62]

Compared to the number of studies on the SME in linear amorphous polymers, the number of studies on this effect in polymer networks is much smaller (see, *e.g.*, Refs 63–67). Most experiments were carried out using epoxide polymers (EP) and by and large revealed the same laws. Namely, recovery of the initial sizes of samples on heating in the free state begins below T_g and completes at $T \approx T_g$, long-term ageing at T_d leads to complete relaxation of ε_{res} and the recovery curves of the samples deformed above and below T_g differ appreciably. The last-mentioned fact indicates a change in the residual strain recovery rate on heating deformed EP (Fig. 8).[36,63] A sample deformed by compression below T_g, always recovers a part of its residual strain below the glass transition temperature (LTR). The sample deformed above T_g exhibits no LTR peak.

The temperatures at which the ε_{res} recovery begins are related to T_d only but not to the relaxation transition temperatures in the glass (T_β, T_γ, *etc.*).[36] At the same time the onset of shape recovery correlates with T_g.[64,65] An analogous correlation was also established for the maximum stress developed on heating oriented samples with fixed ends.[64,65] Polymer networks (in contrast to linear amorphous polymers) have a narrower temperature interval of shape recovery. The maximum stress developed in this case increases with an increase in the degree of deformation and in the effective node density of the network.[65,67]

Shape-memory glassy polymers have found wide practical applications. For instance, they are used for the production of thermally shrinkable films utilised as packing material, thermally shrinkable insulating sleeves, details and profiles in the compressed state (convenient for tranportation), rivets and fittings for all-in-one-type adhesive couplings for pipes.[68–76] In particular, such fittings made of EP (first of all couplings) allow fabrication of strong and pressure-tight constructions made of various (including different-type) materials that withstand high internal pressures of gas and liquids.[74,77–80] This is achieved by using a specific epoxy adhesive along with the thermally shrinkable coupling made of a material which possesses a good adhesion towards various substrates. The temperature–time regimes of coupling shrinkage and adhesive hardening are chosen in such a way that shrinkage be followed by hardening; this precludes formation of adhesive-free spots, thus forming a very thin adhesive layer which provides a joint of maximum strength.

Physical ageing processes in polymers are closely related to the SME.[15] The ageing is considerably enhanced with oriented polymers.[81] Therefore, to solve the ageing problem, it is neccessary to know specific features of manifestation and the mechanism of the SME in such polymers. Often, solving particular engineering problems requires suppression of the SME.[82,83]

III. Crystallisable polymers

1. Amorphous-crystalline homopolymers

In contrast to the amorphous polymers mentioned above, the molecular orientations of both phases in amorphous-crystalline homopolymers can be locked at temperatures above the T_g of the amorphous phase because the stability of the orientation is determined by the network of crystalline domains. These homopolymers exhibit a more complex relation between the degree of molecular orientation and stability of oriented materials. Enhancement of molecular orientation can lead to formation of a structure with a high degree of continuity, which improves the stability in spite of high internal stress.[14] The SME occurring with an increase in temperature is due to (i) structural rearrangement of the amorphous phase with possible crystallisation of this phase; (ii) destruction and recrystallisation of crystallites with imperfect shape, (iii) thickening of crystalline blocks and (iv) melting of the crystalline phase.

The SME mechanisms considered in the study,[15] taking thermal shrinkage as an example, are based on such molecular ordering models as transformation of the paracrystalline phase into the crystalline phase; transformation of crystallites with extended chains into crystallites with packed chains; melting of crystallites; disorientation of amorphous regions followed by crystallisation and some other mechanisms. The authors[15] give no preference to a particular thermal shrinkage mechanism but seem to highlight the mechanisms based on the fibrillar structure models,[84,85] which allow quantitative description of the process.

In spite of the numerous publications concerned with the SME in amorphous-crystalline homopolymers (including recent communications[16,86–101]), investigations of this phenomenon are far

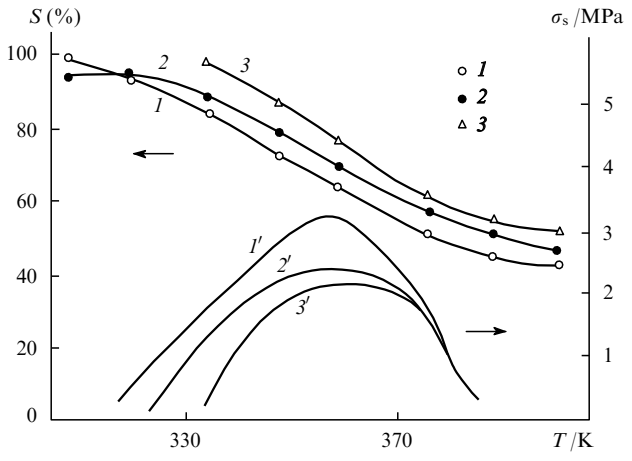


Figure 9. Degree of shrinkage (*1*–*3*) and shrinkage stress (*1′*–*3′*) of LDPE plotted *vs*. temperature.[89]
T_d /K: 293 (*1*, *1′*), 313 (*2*, *2′*) and 333 (*3*, *3′*); $\lambda = 4$.

from being completed. At the same time a number of undoubtful facts and laws were established, which are common to these materials. As a rule, they concern thermal shrinkage of film or block samples, mainly polyolefins. A typical example is shown in Fig. 9 where the degree of shrinkage, S, of low density polyethylene (LDPE) samples oriented by hydrostatic extrusion is plotted *vs*. temperature [89]

$$S = \frac{l_0 - \Delta l}{l_0},$$

where l_0 is the initial length of extrudate and Δl is the shrinkage due to annealing. The shrinkage increases with an increase in the annealing temperature and with a decrease in T_d. Similar results were obtained for polyethylene and polypropylene (PP) films.[88, 102] As in the case of glassy polymers, the shrinkage onset temperature of oriented crystallisable polymers decreases as the degree of deformation increases.[86, 90–92]

Heating of LDPE samples with fixed ends to 350–355 K is accompanied by an increase in σ_s. Then, σ_s somewhat decreases and dramatically decreases after transition of the material to the molten state (see Fig. 9). The maximum values of shrinkage stress σ_s^m increase with an increase in the degree of extension, λ, and with a decrease in T_d (Fig. 10). Shrinkage stress disappears if samples are aged at $T \geqslant 388$ K, which approximately corresponds to the melting completion temperature of crystallites in oriented LDPE [according to differential scanning calorimetry (DSC) data].

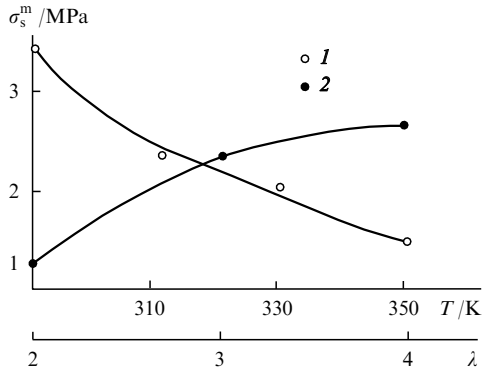


Figure 10. Maximum shrinkage stress of LDPE plotted *vs*. temperature of deformation (*1*) and degree of molecular chain extension (*2*).[89]
$\lambda = 4$ (*1*) and $T_d = 313$ K (*2*).

A study [89] of LDPE extrudate morphology showed that deformation is accompanied by formation of layered structures (crystalline lamellae arranged normal to the extension direction). As T_d increases, the lamellae become thicker. Macromolecular fragments in the bulk of the crystallites that form layered structures acquire now a preferred orientation along the deformation direction. Shrinkage forces (entropic in character), which are developed in thus formed strained throughout-going chains or their clusters, are compensated by elastic forces in the layered crystalline cage. Heating of oriented LDPE samples is accompanied by shrinkage of extended macromolecules or their fragments under the action of entropic factors by transformation of the crystalline cage; this is the reason for such a molecular shrinkage.

Maxima of σ_s are observed in the temperature interval 358–363 K (see Fig. 9) corresponding to completion of the α-transition in LDPE.[103, 104] On further heating the forces that hold the shrinking throughout-going chains within the block become weaker than the forces necessary for block displacement. As a result, chain slip through lamellae begins, resulting in a decrease in σ_s. The higher the temperature, the easier the slip of macromolecular fragments. Therefore, the number of strained throughout-going chains decreases with an increase in T_d, thus leading to a decrease in both σ_s and the degree of shrinkage. The latter is first of all due to the disappearance of the strained throughout-going chains in defect crystallites whose breakdown requires the lowest activation energy. Owing to the absence of low-temperature relaxators, the beginning of the shrinkage process is shifted towards higher temperatures (see Fig. 9). At the same time DSC data show that the shift of the σ_s maximum towards higher temperatures with an increase in T_d is due to the formation of the layers comprised of crystallites with increased cross sections (breakdown of these particles requires a higher activation energy).

Yet another factor responsible for structural rearrangement on heating of oriented LDPE samples, is thickening of lamellae during annealing. In this case certain segments can be drawn into the lamellae, thus leading to disordering of crystalline blocks and development of internal stress. This mechanism can also contribute to an increase in σ_s for the samples oriented at low temperatures. Namely, as T_d increases, partial annealing does occur, as indicated by the thickening of lamellae.[89]

Of particular interest is the investigation of the SME in microporous crystallisable polymers, which are widely used for, *e.g*., filtration, separation of liquid media, deaeration, *etc*. Shrinkage of microporous high-density polyethylene (HDPE) films prepared by melt extrusion, subsequent annealing at fixed size, uniaxial extension during pore formation stage and thermal fixation of porous structure was studied.[94, 95] Correlations between the shrinkage and the draw ratio, temperature of thermal fixation and the degree of extension (ε) were established.

The dependence of shrinkage on the degree of extension passes through an extremum (maximum) at $\varepsilon = 150\%$ whose position is independent of shrinkage temperature.[94] The results obtained were explained by competition between (i) orientational processes (pulling apart and bending of lamellae) and deformation of chains connecting lamellae and (ii) breakdown of the throughout-going chains. At low degrees of extension, the throughout-going chains are not stretched and lamellae are slightly bent. Temperature variation causes strained lamellae held by the throughout-going chains to return to the initial state; however, lamellae (both weakly strained or non-connected by the throughout-going chains) show low deformability; therefore, a small shrinkage is observed at small ε. At $\varepsilon \approx 150\%$, most throughout-going chains appear to be bent and strained, the degree of pulling apart a lamellae becomes high and the connecting chains still withstand the stress. This is the case for maximum shrinkage. At $\varepsilon > 150\%$, a fraction of the throughout-going chains are broken and do not contribute to subsequent relaxation of the sample on heating.

The shape memory effect in microporous films is used in chemical cells. Such films act as membrane separators that are permeable to electrolyte and separate the anode and cathode

compartments.[94, 95, 105] For instance, to avoid ignition of lithium cells, the power source must be prevented from overheating. This is achieved by shrinkage of the separator, which results in closure of through pores and termination of cell operation.

Formation of a network of chemical cross-link points in crystallisable polymers offers additional possibilities of control of thermal-shrinkage characteristics. Such a network can be formed using radiation-induced, chemical or photochemical cross-linking. A hot-drawn polyethylene film prepared by radiation-induced cross-linking exhibits improved ultimate strength, shrinkage stress and a more stable shrinkage factor as compared to non-irradiated film oriented under the same conditions.[106–108] Similarly to the non-irradiated film, shrinkage increases with both an increase in the degree of deformation and a decrease in T_d. A distinctive feature of this material is a characteristic dependence of σ_s, which exhibits a plateau near T_m. For instance, the parameter σ_s of LDPE shows a dramatic increase at $T = 353–383$ K, a constant value to 413–433 K and subsequent gradual decrease.[108]

Photochemically cross-linked and radiation-modified polyolefin samples exhibit a similar shrinkage behaviour.[88] They mainly differ in absolute values of the effects observed. However, this holds for those polymers that were oriented after cross-linking. The situation changes if orientation precedes cross-linking. Exposure to ionising radiation causes a considerable decrease in σ_s, while photochemical cross-linking has little effect on thermal shrinkage. The results of photochemical cross-linking also depend on the nature of initiators employed.[88]

If an amorphous-crystalline polymer contains a network of chemical cross-link points, orientation leads to an increase in the number of throughout-going chains. This is the reason for improved stress-strain properties [88] and increased σ_s. The shrinkage stress determined by the elastic properties of a uniaxially extended network of chemical cross-link points manifests itself in full measure only at $T > T_m$. In the case of radiation-induced cross-linking a large proportion of chemical cross-link points is formed as a result of recombination of radicals that were generated in crystallites and experience a diffusion motion towards relatively ordered transient layers on folded lamellae surfaces.[109, 110] These cross-links can control the degree of 'untwisting' of certain macromolecules and act as additional fixators of crystalline blocks with respect to transfibrillar throughout-going chains, thus precluding chain slip at high temperatures.[88] The density of transient layers, in which efficient radiation-induced cross-linking can occur, is close to the density of crystallites;[111] therefore, they are inaccessible to photoinitiator molecules localised only in amorphous inter-lamellae regions.[112] This is the reason for their different influence on the formation of microfibrillar structure during deformation of cross-linked polyethylene (PE).[88] Lower efficiency of fixation of crystalline blocks on the throughout-going chains, due to inaccessibility of lamellae surfaces to cross-linking in the photoinitiated process, is the reason for insignificant differences between the σ_s regions for the samples cross-linked before and after orientation.

Improvement of the stress-strain and thermal-shrinkage characteristics, achieved as a result of cross-linking of polymers, favours a wide use of polymers in the production of thermally shrinkable items for electronics, the aviation industry, spacecraft industry, automotive industry and the shipbuilding industry.[113] Not only one-layer thermally shrinkable insulating sleeves but also two-layer coatings made of polymeric materials with different properties and different functions have come into use.

2. Copolymers

The synthesis of copolymers is an efficient method of modification of polymer structures and expansion of their functional possibilities. Among recent publications concerned with the SME in copolymers, we will first of all point out the studies of thermoplastic polyurethanes (PU).[114–136] Increased interest in these materials is due to relatively low cost, good processability, high stability to the surrounding atmosphere, convenient (for practical applications) shape-memory temperature intervals and the high degree of shape recovery of PU.

Segmented PU having an SME-appropriate structure were first synthesised by researchers at Mitsubishi Heavy Industries (Japan)[115, 116] from 4,4′-diphenylmethane diisocyanate and polyol using 1,4-butanediol as a chain extender. The structures of these materials consist of soft and hard segments (reversible and 'frozen' phase, respectively). The reversible phase has an amorphous structure while the 'frozen', or fixed, phase has a crystalline structure. In the temperature range between the glass transition temperature and the melting temperature of the crystalline phase, the polymers are in the rubbery state. Deformation at $T_g < T < T_m$ followed by cooling under load to $T < T_g$ causes fixation of the shape acquired. If the material is then again heated to a temperature in the range $T_g < T < T_m$, the initial shape is recovered.

These materials exhibit not only shape memory but also a considerable change in the elastic modulus near the glass transition temperature. This is suggesting of elasticity memory,[116] which is widely used in temperature sensors, drives, low-power engine chokes, *etc*.;[115, 116] therefore, it is of great importance to know the behaviour of such materials in cyclic tests.

Figure 11 presents the residual and recoverable (ε_r) strain plotted *vs*. number of load/unload cycles (N). The data were obtained in the extension of oligoester polyol PU samples characterised by a high elastic modulus at elevated temperatures.[115] Each cycle in the experiment included loading at a constant rate until maximum deformation, ε_m, at 338 K (T_g = 318 K) followed by cooling to 298 K under load and subsequent unloading. Initially, the ε_{res} and ε_r values differ appreciably (see Fig.11). As N increases, ε_{res} also increases and ε_r decreases; the greatest changes are observed at $N < 5$. At $N > 20$, the differences between ε_{res} and ε_r become small and the parameters remain practically unchanged on further cycling. Therefore, attainment of constant ε_{res} and ε_r values for this material requires cyclic preloading (5–20 cycles).

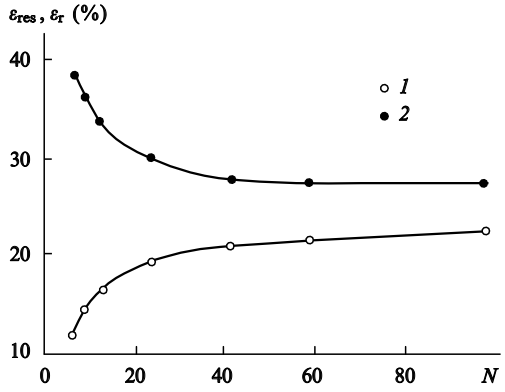


Figure 11. Residual (*1*) and recoverable (*2*) strain plotted *vs*. number of load cycles for PU.[115]

The parameter ε_r of the PU in question can be as high as hundreds per cent; however, most shape-memory elements operate in the recoverable strain region (< 20%).[116, 129] This is due to the fact that the SME is often imparted by bending deformation. Even at $\varepsilon > 3\%$, a nonlinear deformation can begin, which must be taken into account in the design of shape-memory elements.[128] A reference thermomechanical model proposed [128] with allowance for this fact includes nonlinear stress terms in the elastic and viscous components of the linear model.[130]

Plastic deformation recovery in the unloaded state is described by the following equations [130]

$$\dot{\varepsilon} = \frac{\dot{\sigma}}{E} + \frac{\sigma}{\mu} - \frac{\dot{\varepsilon} - \varepsilon_{ur}}{\lambda} + \alpha\dot{T}, \qquad (7)$$

$$\varepsilon_{ur} = S\varepsilon_{res}, \tag{8}$$

where E, μ, λ, and α are respectively the elastic modulus, viscosity, delay time and thermal expansion factor, ε_{ur} is the unrecoverable strain, and S is the coefficient of proportionality. With inclusion of nonlinear terms one has

$$\dot{\varepsilon} = \frac{\dot{\sigma}}{E} + m\left(\frac{\sigma - \sigma_y}{k}\right)^{m-1}\frac{\sigma}{k} + \frac{\sigma}{\mu} + \frac{1}{b}\left(\frac{\sigma}{\sigma_c} - 1\right)^m - \tag{9}$$

$$- \frac{\varepsilon - \varepsilon_{ur}}{\lambda} + \alpha\dot{T},$$

$$\varepsilon_{ur} = S\left(\varepsilon_c + \varepsilon_p\right), \tag{10}$$

where σ_y is the yield stress; σ_c is the stress corresponding to ε_c; ε_c is the unloading deformation of the sample; and ε_p is the time-independent plastic deformation. The results of calculations [128] show that the model gives a correct description of the $\sigma - \varepsilon$, $\sigma - T$, $\varepsilon_r - T$ and other dependences.

Figure 12 presents the temperature dependences of ε_r calculated for different heating rates of unloaded oriented PU samples.[128] Deformation recovery slows down with an increase in temperature, but the ε_{ur} rapidly increases at $\dot{T} > 0.1$ K s^{-1} (Fig. 13). This feature must be taken into account in the design of bulk shape-memory elements for operation under rapid heating conditions because heating of surfaces to a preset temperature does not ensure the SME in the bulk of the material.

Kim *et al.*[126] reported polyurethanes with crystalline hard segments from the reaction of 4,4′-diphenylmethane diisocyanate and 1,6-hexanediol and amorphous soft segments from the reaction of hexamethylene diisocyanate and 1,2-butanediol and studied their thermal, stress-strain and physico-mechanical properties and the SME in this type of PU. First, the materials show sharp glass-transition temperatures that could be used as shape-recovery temperatures. Second, as the block lengths decrease, phase mixing increases and hysteresis in the shape-memory behaviour decreases. Third, too low a content of hard segments (shape-'memorising' phase) increases the hysteresis in the shape-memory behaviour.

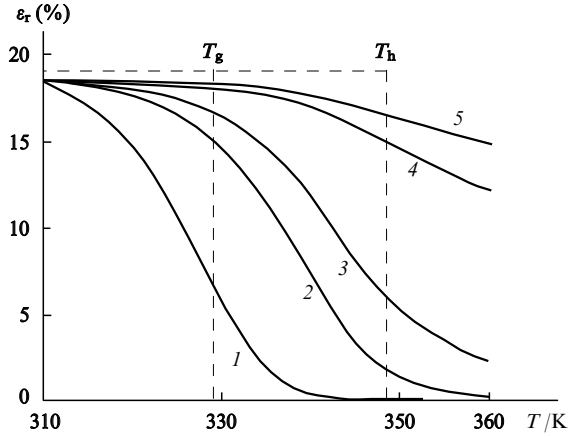


Figure 12. Temperature dependences of recoverable strain for PU.[128] $\dot{T}$/K s^{-1}: 0.0167 (*1*), 0.0833 (*2*), 0.167 (*3*), 0.833 (*4*) and 1.67 (*5*).

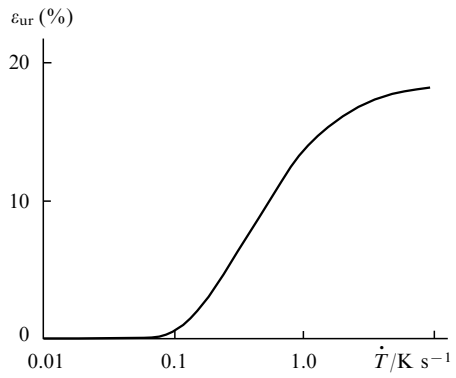


Figure 13. Dependence of unrecoverable strain on the heating rate for PU.[128]
$T = T_h$ (see Fig. 12).

New information on the behaviour of segmented PU with a reversible amorphous phase was reported by Chun and co-workers.[127] who studied a material with diphenylmethane diisocyanate hard segments and poly(tetramethylene glycol) soft segments. The shape retention of PU samples with 30 mass %, 35 mass %, 40 mass % and 45 mass % of hard segment content was estimated after they were deformed by 50% at $T = T_g + 20$ K, cooled under load at $T = T_g - 20$ K and then unloaded. All the tested samples showed more than 90% shape retention. Shape recovery measured after the samples were kept at $T = T_g + 20$ K with load removed varied from 80% to 95%. However, shape recovery was not observed at 20 mass %, 25 mass % and 50 mass % of hard segment content. This behaviour was associated with the character of intermolecular interactions between PU segments. The high degree of shape recovery at $T > T_g$ is due to PU stabilisation by dipole–dipole interactions, hydrogen bonds and induction interactions between the hard segments. The PU samples with 20 mass % and 25 mass % of hard segment content cannot have strong intermolecular interactions and physical cross-links due to the low proportion of hard segments, which results in the loss of shape memory effect. At a hard segment content of 50 mass %, intermolecular interactions between them are strong enough to form a rigid structure, which is inappropriate for SME to occur.

Polyurethanes with the glass transition temperature of the soft segments close to room temperature have found wide application. They are characterised by a stepwise change of many parameters near T_g. The shape-memory function underlies the operation of studs, catheters, fittings, re-writable compact disks, implants for cardiology, *etc.*[136–138]

Crystallisable soft segments can also play the role of the reversible phase in segmented PU. A schematic illustration of the SME in segmented PU with both crystallisable phases and corresponding evolution of the polymer structure is shown in Fig. 14.[117] Crystalline regions formed by hard segments play the role of physical cross-links while soft segments can 'freeze' rubber-like elastic deformation. Initial samples can show microphase separation and both types of segments can crystallise separately with random distribution of crystallites over the sample without any macroscopic anisotropy. In this case at temperatures above the melting temperature, T_{ms}, of soft-segment crystallites but below the melting temperature, T_{mh}, of hard-segment crystallites, the sample is in the rubbery state. Samples can recover their initial sizes even at a high degree of extension. However, isometric cooling of extended samples down to low temperatures makes it possible to 'freeze' and retain the rubbery elastic deformation owing to crystallisation of soft segments. Reheating of such samples leads to melting of soft-segment crystallites and the elastic energy stored causes recovery of the initial geometric sizes.

According to the concept of existence of soft-segment and hard-segment crystalline regions, the crystal perfection, crystalline phase morphology and, hence, crystallisation conditions must significantly influence the shape memory of polyurethane samples. For instance, taking PU prepared from 4,4′-diphenylmethane diisocyanate and toluene diisocyanate and containing caprolactone soft fragments as an example, it was established [117] that some weak cross-links in the samples are broken after the first cycle of deformation, which results in the formation of a dynamically perfect elastic network capable of nearly complete shape recovery. Samples with short soft segments and low hard segment content exhibit small recoverable strain. Long soft segments and

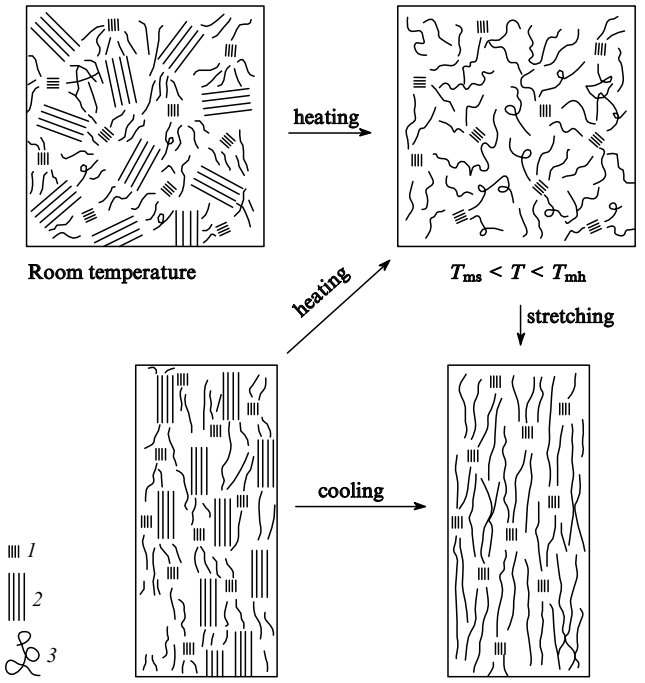
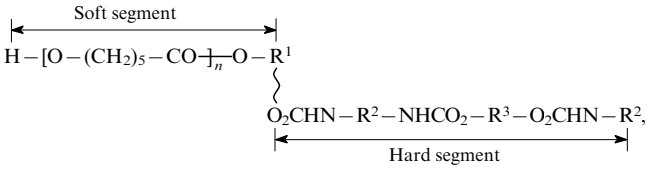


Figure 14. Schematic illustration of the SME in segmented PU.[117] Hard-segment crystallite (*1*), soft-segment crystallite (*2*) and non-crystalline region (*3*).

high hard segment content provide a high degree of shape recovery, namely, 93% – 98%.[119]

Kim *et al.*[121] studied a total of fifteen types of segmented PU with crystallisable soft segments of the type



and concluded that the characteristics responsible for SME are closely related to the mechanical properties of the material. Large elastic moduli of glassy PU favour high shape fixity upon cooling and unloading. At the same time large rubbery-state moduli provide a high degree of shape recovery on heating and storage at high temperatures. If shape fixity is high, precise shaping is possible. High degree of shape recovery leaves small hysteresis in the plots of temperature dependences, which is desirable for shape-memory polymers. At the same time the glassy and rubbery-state moduli strongly depend on the length and concentration of soft segments. Elongation of soft segments during crystallisation causes both moduli to increase and an increase in the soft segment content leads to an increase in the glassy modulus and a decrease in the rubbery-state modulus. The increase in the glassy modulus is due to an increased phase separation, while the decrease in the rubbery-state modulus is mainly caused by a decrease in the hard segment content.

The SME in segmented PU also depends on the sample preparation conditions. It was shown [122] that T_d has virtually no effect on the recovery rate and temperature at $T_d = T_{ms} + (10-30)$ K. Samples deformed at $T_d = T_{ms}$ show lower recovery rate and temperature compared to those found at $T_d > T_{ms}$. An increase in the degree of extension has a minimum effect on the shape recovery temperature, whereas the rate and degree of recovery appreciably decrease at $\lambda > 3$. As the time of keeping the sample at T_d increases, these parameters also decrease, but the shape recovery temperature remains unchanged. The results obtained can be explained by the fact that the response temperature of shape memory is dependent on the melting temperature of the soft segment crystals but the degree and rate of recovery are related to the change in stability of hard segments under stretching and to the hard segment content in the copolymer.

The synthesis of segmented copolymers appeared to be quite promising for thermally stimulated SME. For instance, a segmented ethylene oxide – ethylene terephthalate copolymer with long soft segments was synthesised.[139] It was established that at constant hard segment poly(ethylene terephthalate) content, an increase in the molecular mass of soft segments poly(ethylene oxide) favours their crystallisation. At the same time an increased hard segment content at a constant molecular mass of soft segments hampers this process. These features of soft segment crystallisation influence the character of the strain recovery curves, namely, the higher the hard segment content and the molecular mass of soft segments, the larger the ε_r value. An increase in the hard segment content at a constant length of soft segments also causes the recovery rate to increase. Therefore, the SME parameters can be controlled by varying the hard segment content and soft-segment molecular mass. An increase in the degree of extension reduces the strain recovery degree and rate.[140] Longer orientation process times also lead to undesired results for these characteristics, which can be explained by rupture of physical cross-links formed by the hard segments.

The shape-memory behaviour of this segmented copolymer is very similar to that of the segmented PU [119, 122] analysed above, which allows it to be considered common to this type of polymeric materials. However, comparison of the results of cyclic strength tests for segmented polyurethanes [115, 121, 133] and segmented polycaprolactone – polyamide block copolymers showed that this coincidence is not necessarily true.[140] If the shape of the $\sigma - \varepsilon$ curves for PU varies on cycling and the residual strain corresponding to the beginning of the second and subsequent loading cycles increases, the polycaprolactone – polyamide systems do not show similar changes on cycling. Different shapes of the $\sigma - \varepsilon$ curves of the systems under comparison are due to the fact that redeformation of PU causes mixing of the soft and hard phases and segmental orientation,[141] which is not observed in the polycaprolactone – polyamide block copolymers.

The shape-memory copolymers considered in this Section exhibit two features. These are the presence of (i) trigger segments characterised by a temperature transition within a certain temperature interval ($T_g < T < T_m$ or $T_{ms} < T < T_{mh}$, depending on the structural organisation of segments) and (ii) cross-links responsible for shape retention. All the results listed above were obtained in studies of thermoplastic polymers. The synthesis of polymer networks with analogous functions opens new possibilities of shape-memory control. For instance, the shape-memory behaviour of a polymeric system based on oligo(ε-caprolactone)dimethacrylate, which plays the role of crystallisable trigger segment, and n-butyl acrylate (the content of this component is determined by the density of cross-links) was investigated.[142] The authors studied the effect of the molecular mass of oligo(ε-caprolactone)dimethacrylate and the content of n-butyl acrylate on the thermocyclic behaviour and thermomechanical properties of the material. It was shown that an increase in the content of n-butyl acrylate causes an increase in the degree of shape recovery from 93% to 98%, but the shape fixity decreases. Both the molecular mass of oligo(ε-caprolactone)dimethacrylate and n-butyl acrylate content strongly affect the physico-mechanical properties of the network. In particular, an increase in the content of comonomer leads to a decrease in the elastic modulus at elongation and increased plasticity. The SME was exemplified by a spiral which changed its shape to a rod (permanent shape) within a 20 s period at 343 K. Due to biocompatibility of the components, this material has found applications in medicine.

Graft copolymers are considered as promising shape-memory materials along with the segmented copolymers. Studies [143] of the PE – nylon-6 system with nylon content of 5 mass % – 20 mass % showed that the role of physical cross-links is played by the nylon domains of size at most 0.3 μm, dispersed in the polyethylene matrix. All the samples studied showed good shape recovery (the degree of shape recovery exceeded 95%). The recovery rate was comparable with that of irradiated polyethylene with a high density of chemical cross-links. However, it should be noted that these graft copolymers contain a certain proportion of chemical cross-links because of the use of initiator (dicumyl peroxide) in the course of sample preparation. Since the density of cross-link points is low, it is the nylon domains that are responsible for excellent shape-memory behaviour of the material. The authors proved this statement by the results of their study,[144] according to which, at a low density of chemical cross-links in PE, this component shows no necessary shape-memory characteristics. In particular, the strain mainly remains irreversible.

As in the case of homopolymers, radiation-induced cross-linking improves the properties of shape-memory copolymers. For instance, taking modified PE obtained by copolymerisation of ethylene with octene as an example, it was shown [145] that exposure to γ-radiation (at relatively low absorbed dose) leads to the formation of a material suitable for the production of thermally shrinkable items with a long working life. This material can remain in a stressed state more than 10 years after the origination of shrinkage stresses in it. At the same time the initial shrinkage stress of this radiation-modified copolymer is 1.3 and 1.9 times higher compared to HDPE and LDPE, respectively.

IV. Polymer blends and filled polymer composites

Polymer mixing techniques allows a gradual variation of their physico-mechanical properties including the SME parameters (recovery temperature and rate; shape fixity; stress developed during shape recovery, *etc.*).[146] Nevertheless, only a few studies on the SME in polymer blends are available. Among the reports published in the last decade, mention may be made of the studies [147–154] concerned with various methods for preparation of this class of materials with desired characteristics.

The authors of the studies [147, 148] (see †) used blends of thermoplastic PU having soft polycaprolactone segments, with PVC and phenoxy resin. It was established [147] that the structure of PU – PVC blends comprises amorphous domains of the mixed PVC – polycaprolactone phase and crystalline domains formed by the hard segments of PU. Partial mixing of the soft and hard segments increases as the polycaprolactone segments are shortened. The glass transition temperature of the mixed phase gradually varies as the blend composition changes. Although these variations are small, the initial shape recovery temperature of this polymer system is lower than that of PVC. Cyclic tensile tests of the PU – PVC samples (2 : 8 molar ratio) showed a smaller hysteresis compared to PVC. At the same time the samples with a 4 : 6 molar ratio of the components exhibited an increase in the residual deformation compared to PVC. This behaviour is associated with a change in the elastic modulus in the glassy and rubbery states caused by the variation of the blend composition.

The glass transition temperature of the system PU – phenoxy resin [148] (here, the amorphous mixed domain is formed by the polycaprolactone segments) also gradually changes depending on the component ratio, similarly to the PU – PVC system. Hysteresis in the shape recovery decreases with an increase in the hard segment content and with shortening of these segments, because a highly dispersed distribution of the hard segments constituting the 'frozen' phase favours better 'memorising' of the initial shape.

† These studies are in essence a continuation of earlier studies [123–126] on shape memory effect in segmented PU.

Polymers based on interpenetrating polymer networks (IPN) whose components strongly differ in hardness exhibit a specific deformation and shape recovery (shrinkage) behaviour. The results of studies [64, 65] carried out using a polyurethane – polyesteracrylate (PU – PEA) system suggest that orientational hardening affects mainly the elastic component, PU. Hardening is due to the fact that the hard network (PEA) precludes relaxation of the stressed PU chains by forming macromolecular entanglements each acting as a kind of stopper. At low PEA content, the deformation hardening is insignificant because the density of entanglements is low and the elastic component can relax with ease. As the PEA content increases, the degree of the orientation hardening also increases, but at a PEA content of nearly 30 mass % mechanical degradation processes begin, involving both the elastic and hard chains.

The temperature interval corresponding to the characteristic change in σ_s of the IPN studied (Fig. 15) indicates the domimant role of the elastic component. The decrease in the half-width of the $\sigma_s(T)$ maximum with an increase in ε points to a simultaneously increasing contribution of destructive processes (materials with imperfect structure break down faster in the course of σ_s measurements). As ε increases, the height of the $\sigma_s(T)$ peak varies non-monotonically (not shown in Fig. 15) and passes through a maximum. This behaviour of σ_s is associated to the network loosening and partial stress relaxation in the samples tested and kinks in the right branch of the bell-shaped $\sigma_s(T)$ curve are related to the contribution of the hard component.

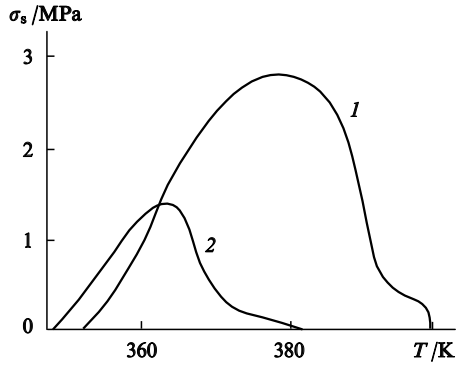


Figure 15. Temperature dependences of shrinkage stress for PU – PEA (70 : 30) blend.[65]
ε (%): 25 (*1*) and 40 (*2*); T_d = 358 K.

PE – PP blends are the most widely studied polymeric systems. In spite of the thermodynamic incompatibility of these polymers the stress-strain properties of their blends at small deformations (small extension) change in additive fashion depending on the blend composition.[155–157] At large deformations, deviations from the additive behaviour of the parameters are observed (decrease in ductility is particularly pronounced [156]). This is due to a weak interphase interaction between the components.[152, 155] To avoid undesired results, various methods are used, *e.g.*, photochemical cross-linking.[52] Figure 16 presents the temperature dependences of σ_s obtained for photochemically cross-linked LDPE films and for LDPE – PP (50 : 50) blend films deformed at room temperature. To reveal peculiarities of the behaviour of blends with different component ratios the temperatures were specified, corresponding to the onset of shrinkage (T_1), maximum shrinkage stress (T_2) and kinks associated with the melting temperature (T_3). The σ_s peak is observed in the pre-melting region of the polymer blend. The parameter σ_s decreases due to slip of certain stressed chains between crystalline blocks ('holders'). In contrast to non-cross-linked samples, the cross-linked ones retain a certain level of σ_s at temperatures above T_m owing to the elastic properties of the network. As the PP content in the blend increases to 50 mass %,

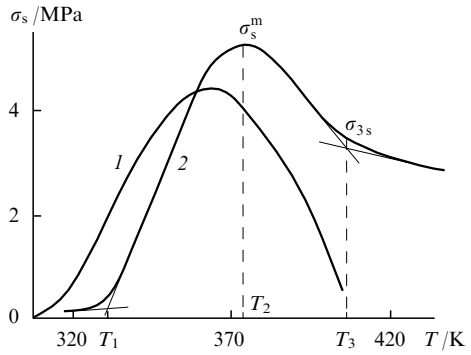


Figure 16. Temperature dependences of shrinkage stress for LDPE (*1*) and LDPE – PP (50 : 50) blend (*2*).[152]

the σ_s^m and σ_{3s} values and the characteristic temperatures (T_1, T_2, T_3) increase (Table 1) and the samples exhibit shape-memory behaviour at $T > T_3$ (T_3 much exceeds the melting temperature of LDPE) . Thus, introduction of PP into LDPE followed by cross-linking of the blend favours retardation of relaxation processes in the oriented samples.

Table 1. Thermal shrinkage characteristics of photochemically cross-linked oriented LDPE – PP blends.

$\frac{[LDPE]}{[LDPE]+[PP]}$	T_1 /K	σ_s^{max} /MPa	T_2 /K	σ_{3s} /MPa	T_3 /K
1.0	47	4.4	86	0.97	122
0.9	48	4.45	87	1.56	124
0.8	48	4.52	87	2.04	125
0.7	52	5.13	91	2.89	127
0.5	54	5.30	96	3.35	129

To attain rather high degrees of extension in creating orientation order in LDPE – PP blends, hydrostatic extrusion was employed.[151] The technique permits nondestructive deformation of brittle materials. Similarly to cross-linked film samples,[152] LDPE – PP extrudates lose the shape at higher temperatures compared to LDPE samples (the higher the PP content, the better the shape fixity). The degree of shape recovery was estimated [151] from the change in the extrudate cross sections on heating

$$\Psi = \frac{d_h^2 - d^2}{d_h^2},$$

where d and d_h are the extrudate diameter before and after heating. It was established that the dependences of Ψ on the degree of extension λ in the whole temperature interval studied are non-monotonic and pass through a maximum near $\lambda = 3-4$. Both the λ value corresponding to the extremum and the respective Ψ value decrease as the PP content in the blend increases from 0 mass % to 60 mass %. The residual deformation increases as λ increases. This unusual (at first glance) pattern of the $\Psi(\lambda)$ dependence is due to simultaneous action of two factors that cause swelling of an extrudate, namely, relaxation of viscoelastic deformations in the extrudate at the die outlet and an increase in the cross section of the extrudate on heating owing to the SME. A decrease in the maximum Ψ values and their shift towards smaller λ with an increase in the PP content are due to the lower shape recovery ability of the LDPE – PP blends compared to LDPE and to differences between the die swelling and λ for the materials under comparison.

A study [151] of thermal shrinkage characteristics of samples with fixed ends showed that the characteristic temperatures of thermal shrinkage processes (see Fig. 16) depend only slightly on λ and on the PP content and obey laws identical to those established for the film samples oriented by uniaxial stretching (see Table 1). The σ_s^m values increase with an increase in λ and PP content in the blend. Similarly to the case of cross-linked samples,[152] the process of stress relaxation is not completed at the melting temperature of the polyethylene phase; rather, it extends to a wider temperature range. The shrinkage stress corresponding to this temperature interval (σ_{3s}) increases as λ and PP content increase.

In the preceding paragraph we described the behaviour of monolithic samples of LDPE – PP blends prepared using a Banbury-mill type mixer and orientationally stretched under high hydrostatic pressure. Using the method of plunger extrusion of polymeric powder billet,[158] which combines monolithisation and orientation stretching, the authors [149] prepared and studied samples of PP blends with LDPE and ultra-high-molecular-mass PE (UHMMPE) as well as PVC – UHMMPE blends. For comparison, the behaviour of UHMMPE extrudates prepared by the same technique was studied. It was found that the UHMMPE extrudates behave similarly to homopolymers on heating. Namely, the samples studied showed an increase in diameter accompanied by a decrease in length [*i.e.*, the initial shape (dimension) recovery] at temperatures T such that T exceeds a value of 373 K, being close to the temperature of UHMMPE melting (extrusion) (403 K). The volumes of the extrudates did not change. Relaxation processes in the polymer blends began at lower temperatures compared to the extrusion temperatures of the materials (433 K). For all the systems under study raising the heating temperature was accompanied by monotonic increase in the sample diameters and an unusual change in the degree of shrinkage. An increase in the length of the sample at the beginning was followed by its sharp decrease as a temperature close to the melting temperature of one of the components was achieved. According to calculations, these changes in the size of the sample cause an increase in volume (Fig. 17). The maximum value of the relative change in volume, $(V - V_h)/V$, where V and V_h are the extrudate volumes in the initial state and after heating to a preset temperature, lies in the concentration range corresponding to equal mass fractions and nearly equal volume fractions of the

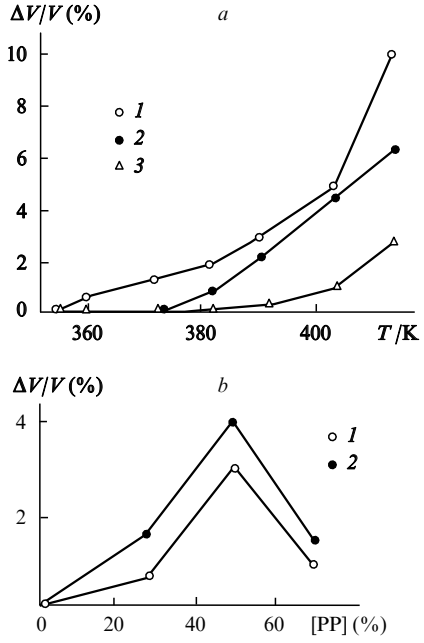


Figure 17. Relative change in volume of polymer blends plotted *vs.* temperature (*a*) and concentration (*b*).[149]
(*a*): PP – UHMMPE (60 : 40) (*1*), PP – UHMMPE (70 : 30) (*2*) and PP – PVC (40 : 60) (*3*); (*b*): PP – UHMMPE blend, $\lambda = 2$; T_h, K: 383 (*1*) and 393 (*2*).

components. The maximum increase in volume is attained at $\lambda = 2$.

The observed increase in volume is related to stress relaxation during the shape recovery process, accompanied by the appearance of discontinuities at interfaces. The anomalous increase in the extrudate length on heating was explained in terms of a model for extrusion of a two-phase composite, which is based on the self-consistent field approach.[159] The model assumes that the two-phase composite has a matrix–inclusion structure. The total deformation of a composite is given by [149]

$$\varepsilon_l = \delta\left(1-\delta\right)\left(\varepsilon_l^m - \varepsilon_l^i\right)^2, \quad (11)$$

where δ is the relative volume fraction of the inclusions; $\varepsilon_l^m, \varepsilon_l^i$ are respectively the plastic deformation of the matrix and the plastic deformation of the inclusion. From expression (11) it follows that $\varepsilon_l > 0$ and the maximum ε_l value is attained at $\delta = 0.5$, *i.e.*, the maximum stretching must be observed at a volume fraction of inclusions of 50%, which is consistent with experimental data (see Fig. 17).

A DF-10 composite based on polyarylate and copolyethersulfone also exhibits unusual behaviour during the heating of samples prepared by plunger extrusion of polymeric powder billet.[160] The shrinkage, S, defined as the relative change in the extrudate length after keeping at a preset temperature, decreases with an increase in λ and changes its sign near $\lambda = 4$. In other words, the length of the sample increases rather than decreases at a high degree of extension. A scheme illustrating deformation of macromolecular coils in the case of solid-phase extrusion was proposed.[160] According to this scheme, shrinkage is due to return of macromolecular coils to the initial state. The degree of return can be estimated as follows

$$\Psi_m = \frac{C_\infty^\perp - C_\infty^\parallel}{C_\infty^\perp}, \quad (12)$$

where $C_\infty^\perp$ and $C_\infty^\parallel$ are the characteristic ratios, C_∞, calculated along the normal and parallel to the extrusion axis, respectively. The parameter C_∞ serves as a measure of the relative flexibility of the macromolecule and of the degree of compactness of the macromolecular coil.[161, 162]

Thermal shrinkage occurs until the macromolecular coil adopts a symmetrical shape, which corresponds to $C_\infty^\perp = C_\infty^\parallel$. Comparison of the parameters S and Ψ_m revealed their similarity in absolute value and an identical type of dependence on λ. Moreover, the $C_\infty^\perp$ and $C_\infty^\parallel$ values calculated from the equation derived [160] invoking the mechanism of plastic deformation of amorphous polymers (see Ref. 163), show inversion of absolute values at $\lambda > 4$.

Recently, considerable attention has been paid to blends of engineering polymers with liquid-crystalline polymers (LCP).[164–169] The addition of LCP improves not only the mechanical properties of thermoplastics but also the corresponding processing conditions. Therefore, interest in these systems in the framework of SME studies is not occasional. Peculiarities of the shape memory behaviour of a HDPE–LCP blend were studied.[153] The LCP was a liquid-crystalline copolyester of 40% PETP with 60% of 4-hydroxybenzoic acid. Stretching of samples was preceded by radiation-induced formation of a network structure in them. The shape memory effect was studied under conditions of isometric heating and cooling; to this end, thermorelaxation stress σ_{tr} (on heating) and thermal shrinkage σ_s (on cooling) were measured.

The samples of HDPE and HDPE–LCP blends containing 5 mass % and 10 mass % of LCP exhibit quite different temperature dependences of σ_{tr} and σ_s. Indeed, HDPE shows a dramatic increase in σ_{tr} in a narrow temperature interval near T_m, whereas the blends are characterised by a gradual increase in σ_{tr} over a wide temperature range (from 323 to 423 K for the HDPE–LCP blend containing 10 mass % of the LCP). This behaviour is due to the α- and α'-transitions in the PETP phase of the LCP. At temperatures above 423 K, the σ_{tr} value remains virtually unchanged up to 533 K. The $\sigma_s(T)$ dependence obtained for the blends also differs from the corresponding dependence for HDPE (kinks between 333 and 373 K in the former *vs.* nonmonotonic change in σ_s in the latter case). It is important that the σ_s value of the HDPE–LCP blend containing 10 mass % of LCP is 1.5 times higher than the σ_s value for pure HDPE. As the absorbed radiation dose increases from 50 to 150 kGy, the σ_{tr} and σ_s values increase but then decrease due to accumulation of radiation-induced defects in the material.

Physical modification of polyolefins by cross-linking them with various elastomers is one of the most efficient methods of preparation of thermosetting plastics possessing the properties of both elastomer and plastic, namely, flexibility, high impact toughness at low temperatures, *etc*. This modification technique is also of interest for obtaining shape-memory materials exhibiting the properties mentioned above. In particular, the behaviour of LDPE–ethylene/propylene/diene copolymer (EPDC) blends prepared by chemical (series A) and radiation-induced (series B) cross-linking and then orientationally stretched at 403 K and cooled to room temperature under isometric conditions was studied.[170] Series-A samples showed low σ_{tr} and σ_s values, the former increasing with an increase in the content of the cross-linked elastomer. Maxima in the σ_s plot were observed at minimum EPDC content in the blend, because their magnitudes are determined by the crystalline phase of LDPE. Series-B samples also exhibited a similar behaviour of σ_{tr} and σ_s, except for much higher absolute values of σ_s (compared to series-A samples) at the same LDPE/EPDC ratios. This is due to the fact that irradiation of samples causes cross-linking in both phases rather than in one phase. As a result, according to scanning electron microscopy data, fibrillisation of the molecular structure occurs.

A study [154] of HDPE–ethylene-propylene rubber terpolymer (SKEPT)–LCP composite was carried out in a continuation of earlier investigations.[153, 170] Here, rubber is mainly introduced in order to improve the elasticity of the material and its adhesive interaction with steel; this is necessary for the improvement of the technical characteristics of the items produced. The effect of SKEPT and LCP on the maximum σ_{tr} and σ_s values can be followed using the plots shown in Fig. 18. With the SKEPT content below 40 mass % the LCP additive allows thermorelaxation and, of particular importance, shrinkage stress to be enhanced.

Long-term serviceability of items made of thermally shrinkable materials depends on the stability of size when stored; being mounted, they must provide sufficient compression stress during their service life. Hence, the reverse deformation effects (in unloaded state) and stress relaxation (when loaded) must be

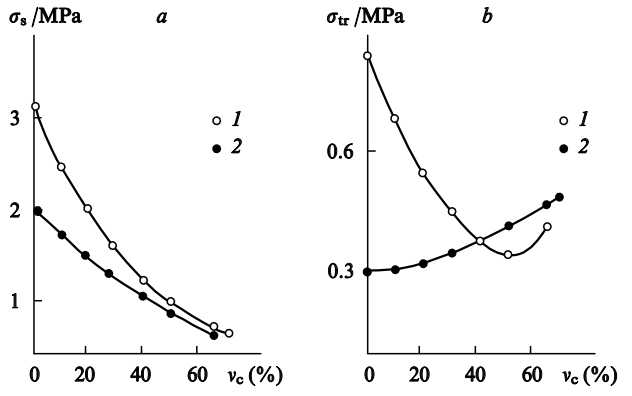


Figure 18. Thermal shrinkage at 293 K (*a*) and thermorelaxation stress at 433 K (*b*) plotted *vs.* SKEPT content in HDPE–SKEPT–10 mass % LCP (*1*) and HDPE–SKEPT (*2*) blends.[154]

small. In radiation-modified PE, the crystalline phase hampers the return deformation. As to HDPE – SKEPT blends, an increase in the SKEPT content causes the proportion of the crystalline phase of PE to decrease, which can lead to shortening of service life. This assumption was tested [153] by measuring the return deformation (with load removed) of radiation-modified (absorbed dose 150 kGy) HDPE – SKEPT and HDPE – SKEPT – LCP samples heated to 423 K and stretched by 100% during cooling to room temperature in the loaded state (with fixed ends).

As samples are released from the clamps, a conditionally instantaneous shrinkage occurs. Subsequent reverse deformation is damping in character. A decrease in the preset extension depends on the material's composition. In particular, the decrease for the HDPE – SKEPT (20 : 80) blend was 33% [*cf.* 8% for the HDPE – SKEPT – LCP (25 : 65 : 10) blend] after 1000 h; *i.e.*, the addition of LCP improved the size stability of the oriented articles. Clearly, the reverse deformation is hampered by not only the crystalline phase of HDPE but also the liquid-crystalline polyester, which acts as a reinforcing agent when oriented.

Few studies on the SME in filled polymer composites are available. This may be due to the fact that the addition of fillers usually deteriorates the operating parameters of SME. Publications [90, 92, 93, 171] are concerned with the shape memory behaviour of polymerisation-filled, UHMMPE-based composites extruded using a process proposed in Ref. 158. The fillers used were aluminum and bauxite. It was established that composites and UHMMPE exhibit qualitatively similar dependences of the degree of shape recovery Ψ, estimated from the change in the cross section of extrudates, on λ. In both cases a nearly linear increase in Ψ is observed as λ increases from 1 to 9. However, Ψ decreases in absolute value in the order UHMMPE – UHMMPE-bauxite – UHMMPE-Al. It was shown that shape recovery is due to rearrangement of the crystalline phase, as indicated by correlations between, *e.g.*, $\Psi(T)$ and the temperature dependences of the degree of crystallinity and between Ψ and an increase in the degree of crystallinity due to orientational stretching.

Thermal shrinkage and molecular orientation of polymerisation-filled composites can be correctly described in the framework of the rubbery elasticity theory, namely, by the Mooney – Rivlin phenomenological equation [171]

$$\lambda_c^m = \left(\lambda^2 - \lambda^{-1}\right)\left(\frac{2C_1 + 2C_2}{\lambda}\right), \qquad (13)$$

where λ_c^m is the degree of molecular orientation corrected for the presence of filler [2] and C_1 and C_2 are constants. In the case of molecular orientation, $C_2 = 0.615$ for UHMMPE – Al (70 mass %) and 0.53 for UHMMPE – bauxite (45 mass %), the corresponding values for thermal shrinkage are 0.015 and 0.030; the C_1 constants are zero in both cases.[171] Since the constant C_1 is associated with the entropy contribution, it was concluded that entropy does not contribute to molecular orientation and thermal shrinkage and that the driving force of these processes is rearrangement of the crystalline phase during solid-phase extrusion. Comparison of the C_2 constants for molecular orientation and thermal shrinkage showed that in the former case the proportion of structural regions involved in the rearrangement is much higher. While molecular orientation occurs involving the whole crystalline phase, thermal shrinkage involves only defect crystallites formed in the course of orientation crystallisation. This also follows from the fractal model for shrinkage.[93]

Conventionally, shape memory effect in polymeric materials is not accompanied by considerable changes in volume. However, as mentioned above, if a porous structure was created in the initial homopolymer billet [34] or discontinuities appeared as a result of internal stress relaxation on heating of oriented polymer blend samples,[149] shape memory effect is accompanied by an increase in volume. This effect can also be achieved by introducing a porous filler, in particular, thermoexpanded graphite (TEG) into the polymer matrix.[172–176] TEG has good compactibility, which allows large deformations to be obtained when fabricating a compact billet. Subsequent heating of the billet will not be accompanied by recovery of the initial dimensions. At the same time, at particular TEG content in the EP – TEG system, it is possible to prepare a composite, which is well-deformable and possesses the ability to complete shape recovery, which occurs on heating to a temperature above the glass transition temperature.

Figure 19 presents the results of a study [175] of cylindrical rods deformed by compression in a mould. Heating of such samples in the unloaded state causes an increase in their length but their diameters remain unchanged. The largest $\Delta l/l$ or $\Delta V/V$ values can reach 45% at a TEG content of 6 mass % – 8 mass %. As the degree of deformation decreases, this interval extends towards higher TEG content.

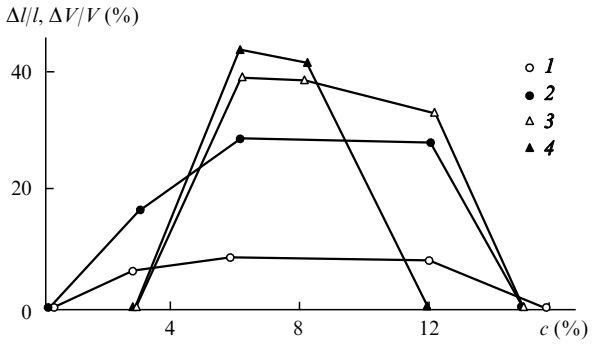


Figure 19. Relative change in length (volume) plotted *vs.* TEG concentration in an EP – TEG system.[175]
ε (%): 10 (*1*), 30 (*2*), 40 (*3*), and 45 (*4*); T_h = 358 K.

Taking into account the results considered above, thermal shrinkage studies of sleeve-shape samples were carried out. It was found that at a TEG content of 6 mass % in the composite, a piped sample can be deformed by up to 60%. On subsequent heating of the sample in the unloaded state the internal diameter decreases to the initial value while the outer diameter and length remain unchanged.

Rod-like articles capable of increasing their diameter with retention of length on heating were prepared using hydrostatic compression of cylindrical billets with fixed ends at 50 – 100 MPa. Such rods can be used for fabrication of disks with radial increase in volume.

By and large, TEG-filled composites based on UHMMPE and PP behave similarly to EP – TEG composites.[175] At the same time, in contrast to the thermosetting composite, the degree of shape recovery for these materials is less than 100% up to the melting temperature of the crystalline phase of the polymer.

A physical model proposed to describe the kinematics of deformation of the porous composite is available.[173, 175, 176] The model was employed to construct the limiting surface of the material in the strain space. The limiting surface restricts the region where the material deforms without failure and represents the surface of a pyramid (Fig. 20). The basal plane, S_0, of the pyramid corresponds to the situation where the material deforms with no change in volume; the plane S_l corresponds to the limiting compaction of the composite; and the *A*-point corresponds to failure of the composite under cubic strain only. The compact material can be deformed only within the S_0 triangle, on the boundaries of which the polymer fails. The porous polymer can be deformed within the truncated pyramid with the bases S_0 and S_l. On the lateral surface of the truncated pyramid, the polymer matrix fails while the upper base corresponds to complete closure of pores.

At a sufficiently high porosity, the S_l plane will move beyond the *A*-point. In this case the reversible strain of the porous composite will be restricted by the pyramid of the limiting surface.

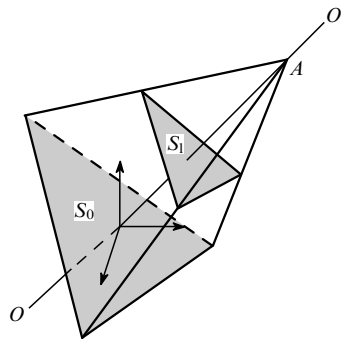


Figure 20. Limiting surface of porous composite in the strain space.[175]

Attempts at further compacting of the material in the stage of initial straining will lead to destruction of the polymer matrix and the recovery of the sample on heating will be incomplete.

Theoretical analysis showed that by prestraining the porous polymer or composite it is possible to form structures which, when recovering their shapes, imitate materials with different (including negative) Poisson ratios (coefficients of proportionality between the longitudinal and lateral strain developed during shape recovery of the sample).

The limiting relative change in the volume of the composite is given by [175]

$$\varepsilon_{\text{lim}} = \frac{\delta_V(1-\theta)}{1+\delta_V}. \qquad (14)$$

Here δ_V is the volume fraction of the filler prior to deformation ($\delta_V = V/V_p$, where V and V_p are the volumes of the porous filler and the polymer matrix, respectively), θ is the relative bulk density of the filler in pores of the composite prior to deformation ($\theta = V_1/V$, where V and V_1 are the volumes of the filler prior to and after deformation, respectively). This relationship shows that the lower the bulk density of the filler, the larger the absolute value of ε_{lim} and, therefore, the farther the S_l plane from the origin. This conclusion is in agreement with experimental results.

From relation (14) it follows that, at a high TEG volume fractions in the composite, the absolute value of ε_{lim} can become so large that the S_l plane will shift beyond the vertex A of the limiting surface. This means that there is a maximum permissible concentration of the carbon material in the composite.

Thermally expanded graphite is a conducting filler; therefore, shape-memory studies of the TEG-filled composites are of particular interest because the carbon material affects peculiar features of the shape memory effect [173–177] while the effect in question in turn affects the conductivity of the composites. Particular attention should be paid to the polymer composites with the nearly threshold filler content, at which the insulator–conductor transition occurs.[178, 179] In particular, being heated, these materials exhibit the effect of self-regulation of the heating temperature, which consists in a dramatic increase in the resistance in a certain critical temperature interval and is due to the thermal expansion of the polymer matrix.[178] However, the range of threshold concentrations is characterised by a very large scatter of resistance values owing to nonuniform distribution of the filler particles over the volume of the matrix, which hampers the attainment of the result mentioned above.[180] This problem can be solved by using those materials which recover their shape with simultaneous increase in volume on heating. Shape-memory behaviour is characterised by a much greater increase in the distances between contacting filler particles that are involved in the conduction process compared to thermal expansion of the polymer matrix. From here one has a wider interval of filler concentrations in which the resistance increases jumpwise.

We studied the resistance of the EP–TEG composite based on diglycidyl phthalate and a block oligomer of aliphatic epoxy resin with acid oligoether cured with isomethyltetrahydrophthalic anhydride. It was established that, at the TEG concentration of nearly 6 mass %, heating of the billets deformed by mould compression causes a sharp increase in the resistance near T_g. The bulk resistivity ratio corresponding to the deformed (ρ_d) and recovered (ρ_r) states can be as high as three orders of magnitude (Table 2).

Table 2. Characteristics of carbon-containing epoxy composites.

Composite	ε (%)	ρ_d /Ω m	$\rho_r \times 10^{-3}$ /Ω m	ρ_r/ρ_d
EP + 3% TEG	20	64 000	502	11
EP + 6% TEG	20	138	60	435
	20	109	60	550
	30	91	60	659
	40	69	60	870
EP + 10% TEG	25	38	10	263
EP + 6% TEG + 2% kaolin	25	154	11	71
EP + 6% TEG + 3% kaolin	25	5.6	4	714
EP + 6% TEG + 4% kaolin	25	90	30	333

Introduction of a binary filler including kaolin powder led to significant changes in the electrical properties of the composite (see Table 2). At the same (with the EP–TEG composite) ε values, the absolute values of ρ_d and ρ_r decrease in the presence of kaolin. The minimum ρ_d value and simultaneously maximum ρ_r/ρ_d ratio were established for the EP–TEG–kaolin (100 : 6 : 3) composite.

Analysis of the strain kinematics and subsequent strain relaxation showed the following. Low bulk density and good compactibility of TEG favour the decrease in the volume of the TEG-filled cavities in the initial cured billet upon deformation due to compression of the filler and filling of the voids thus formed with the polymer. The concentrations of TEG in the composites under study is high enough to ensure the conducting state of the materials, *i.e.*, the presence of a continuous infinite cluster of the filler particles. An increase in the TEG concentration or the degree of deformation of the material causes an increase in the contact area between the TEG particles and thus a decrease in the ρ_d value (see Table 2). When heated to temperatures close to T_g, at which the mobility of the chain fragments between cross-link points of the polymer network unfreezes, the deformed samples recover their shape (their volumes increase) through sample elongation. The polymer leaves pores and TEG remains in the compacted state. Breakage of bonds between the particles of the conducting cluster causes a decrease in the contact area and, as a consequence, an increase in resistance. The process goes to completion when the glass transition temperature is achieved and the shape recovery induced change in the length of the sample ceases.

Microstructural studies showed that the TEG distribution over the bulk of the polymer matrix in the presence of kaolin is more uniform, which favours an increase in the conductivity of the system. The results obtained are consistent with the published data (introduction of kaolin into epoxy polymer filled with graphite also led to a decrease in the system's resistivity).[181] This effect can be used in short-circuit thermal protection, namely, current limiters can be made of a shape-memory material.

V. Polymer gels

Considerable interest [16, 182–196] of researchers in polymer gels as shape-memory materials is due to the fact that their volume can change by three orders of magnitude under the action of external factors (*e.g.*, temperature, solvents, electromagnetic field, *etc.*). Particular attention should be paid to polymer hydrogels in which water molecules fill the intermolecular space of the polymer

network. These materials are soft and 'wet', which improves their compatibility with biological tissues.[186, 187] The shape memory effect underlies the design of temperature-sensitive diaphragms, thermally activating clamps, 'soft' machines and other medical instruments.[186]

The mechanical properties of many water-swollen gels strongly depend on temperature. For instance, a gel prepared by copolymerisation of acrylic acid with n-stearyl acrylate [188] behaves as a hard plastic below 298 K. But at temperatures above 323 K it becomes very soft and can be stretched by 50% relative to its initial length. The elastic moduli of this material decrease by three orders of magnitude on heating, which can be due to reversible order–disorder transition associated with interactions between the alkyl side chains of the stearyl acrylate units. At $T < 323$ K, long alkyl chains form the crystalline structure which reinforces the material. Above this temperature, the material has an amorphous structure, being soft and flexible. It is believed [186] that this mechanism (formation of crystalline aggregates between the side chains) causes the SME in the material.

The gel 'remembers' the shape in which it was initially formed. To show the shape memory, the gel is heated above the transition temperature (323 K), deformed (*e.g.*, stretched or coiled) and then cooled in the deformed state. If the unloaded, deformed gel is again heated, at $T > 323$ K it recovers its initial shape and size in ten seconds.[186] It should be noted that the shape recovery rate and the degree of swelling can strongly depend on the temperature at which the gel was prepared. For instance, at $T_p = 293$ K the degree of swelling of *N*-isopropylacrylamide gel is low ($d/d_0 = 1.2$, where d and d_0 are the diameters of the swollen and freshly prepared gel, respectively). However, as T_p approaches the phase separation temperature (305 K) the d/d_0 ratio considerably increases and then again decreases to 1.46 at $T_p > 305$ K, which correlates with spatial inhomogeneity in the gel.[197] In turn, the shrinking time decreases from 500 min at $T_p \leqslant 293$ K to 2 min at $T_p \geqslant 299$ K.

Spatially modulated polymer gels prepared by restricting interpenetration of gel networks are widely used for fabrication of articles for biomedical applications.[185, 195] These are, *e.g.*, a bigel plate, which can bend and eventually form a ring with an increase in temperature or solution concentration; a gel, which changes its shape from a straight line to a pentagon and then to tetragon depending on temperature; a gel 'hand' which can clench or unclench various material things on temperature variation. The operation of these 'devices' is based on the ability of gels to change their volume depending on the environmental conditions.[198–200] Examples of spatially modulated gels are provided by the systems based on *N*-isopropylacrylamide (IPA) and acrylamide (AAM) gels.[185]

It is known [201] that the volume of ionic IPA gel rapidly decreases at $T > 310$ K, whereas such is not the case for the AAM gel. In turn, it is the AAM rather than IPA gel that shows a large shrinkage in water-acetone mixtures. At room temperature, a completely swollen bigel plate is bent towards the AAM gel. If $T > 310$ K, the plate is gradually bent due to shrinkage of the IPA gel and eventually forms a ring. Being immersed in a water-acetone mixture at room temperature, the plate hoops in the opposite direction but the ring can also be formed. Transition from the linear to a bent shape is reversible and the change in the degree of bending depends only slightly on the number of straightening–bending–straightening cycles, being at most 3% after 9 cycles.

Bending deformation can be estimated from the angle θ between two tangent lines drawn to the ends of the gel arch,

$$\varepsilon = \frac{\theta d}{L},$$

where d and L are the diameter and the length of the gel sample, respectively. The maximum deformation of bigel is 49%.[185] This greatly exceeds the deformation developed in the polyvinyl alcohol–poly(sodium acrylate) system on application of an electric field ($\varepsilon = 20\%$).[202, 203] The kinetics of the shape memory effect in the bigel plate mentioned above can be followed using the plots shown in Fig. 21. Deformation of gel immersed in a high-temperature bath (311 K) increases with time; on cooling to 295 K the bigel gradually recovers its initial shape and size.

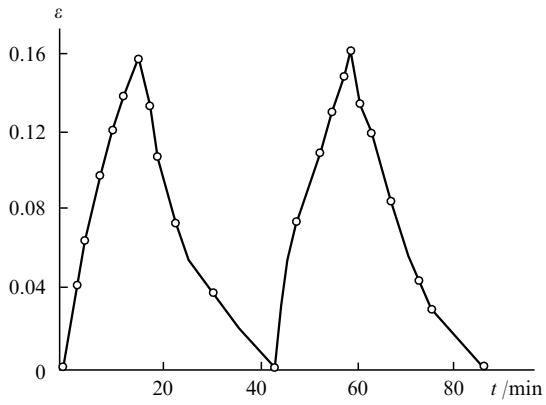


Figure 21. Bending deformation cycles plotted *vs.* time for bigel.[185]

The bigel bending mechanism [185] differs from the mechanisms of shape memory effects induced by electric field [187, 192, 202, 203] or by heating with an IR laser.[184] In the last two cases trigger-type bending of macroscopically homogeneous gels requires the presence of an electric or temperature field gradient. Clearly, these methods are inappropriate to achieve a high degree of deformation ($\theta > 180^\circ$) owing to difficulties in the creation of high field gradients. The thermal expansion coefficients of two gels can differ much more than the corresponding parameters of two metals (*cf.* more than 0.5 per degree for the IPA–AAM bigel *vs.* $\sim 7 \times 10^{-6}$ per degree for a typical brass–steel bimetallic plate; the difference is nearly five orders of magnitude). Therefore, bigels are much more sensitive to temperature changes in the environment compared to bimetals.

Compared to the bigels considered above, gels with a more complex modulated structure allow a variety of reversible transitions to occur. In addition to the 'straight line–pentagon–tetragon' transition (see above), they also include transitions to a sinusoid and helix, a transition from a planar sheet to a tube, *etc.* Such a diversity of transitions at different temperatures is achieved by appropriate modulation of particular regions of the polymeric systems. In this Section we restricted ourselves to illustration of those possibilities of polymer gels that are related to the thermally induced SME. A great body of information on the subject, including modern practical applications and promising projects, was summarised and analysed in a review.[191]

VI. Conclusion

In the last decade, the shape memory effect in polymers has been the subject of intensive research. This provides diverse information on the structure of oriented polymers and mechanisms of their deformation and favours better understanding of the kinetic laws of thermally stimulated relaxation. New studies begin, aimed at the design of polymeric materials offering new possibilities for the shape memory effect to occur; this is important for the extension of the spectrum of practical applications of these materials. Interest in the SME studies is in line with rapid development of research on the so-called 'smart' or 'intellectual' materials including shape-memory polymers. Compared to shape-memory metal alloys, shape-memory polymers offer a number of advantages (low density, high strain-recovery ability, ready processability and dyeability and relatively low cost). It is also important that the SME in polymeric materials occurs at temperatures close to room temperature and in some cases these

materials can be controlled with ease by varying the chemical composition of the polymers.

Among recent achievements, there are considerable advances in studies of the properties (in particular, the LTR mechanism) of glassy polymers;[46–48, 62] preparation of unusual shape-memory polymeric materials (polymer composites with compactible filler,[173, 175] spatially modulated polymer gels [185, 195]); and fabrication of various articles for technological and biomedical applications from shape-memory functional materials.[94, 95, 116, 127, 142] There are also a number of problems that are still to be solved and require further investigations. In particular, the mechanism of SME in amorphous-crystalline polymers is still to be clarified and the mechanism of shape recovery and its relation to the state of the structure of such promising materials as oriented biodegradable polymers [204, 205] and the polymer blends and composites modified by various additives remain poorly studied. Search for new fields of application of shape-memory polymeric materials also remains an important investigation avenue.

Solving problems mentioned above requires further investigations of various aspects of SME in polymeric materials, aimed at gaining a deeper insight into the mechanisms of the shape memory effect, generalisation of experimental data and formulation of practical recommendations for potential users.

References

1. V V Vasil'ev, I G Manets, R A Veselovskii, A A Zolochevskii, Yu S Kochergin *Polimernye Kompozitsionnye Materialy v Gornom Dele* (Polymeric Composite Materials in Mining) (Moscow: Nedra, 1988)
2. A V Chichinadze (Ed.) *Polimery v Uzlakh Treniya Mashin i Priborov* (Polymers in Friction Units of Machines and Instruments) (Moscow: Mashinostroenie, 1988)
3. V U Novikov *Polimernye Materialy Dlya Stroitel'stva* (Polymeric Materials for Building) (Moscow: Vysshaya Shkola, 1995)
4. I I Kornilov, O K Belousov, E V Kachur *Nikelid Titana i Drugie Splavy s Effektom 'Pamyati'* (Titanium Nickelide and Other Alloys with the Memory Effect) (Moscow: Nauka, 1977)
5. A S Tikhonov, A P Gerasimov, I I Prokhorova *Primenenie Effekta Pamyati Formy v Sovremennom Mashinostroenii* (Use of the Shape Memory Effect in Modern Machine-Building) (Moscow: Mashinostroenie, 1981)
6. V N Khachin *Pamyat' Formy* (Shape Memory) (Moscow: Znanie, 1984)
7. V A Likhachev, S L Kuz'min, Z P Kamentseva *Effekt Pamyati Formy* (Shape Memory Effect) (Leningrad: Leningrad State University, 1987)
8. K Otsuka, K Simidzu, Yu Sudzuki, Yu Sekiguti, Ts Tadaki, T Khomma, S Miyadzaki *Splavy s Effektom Pamyati Formy* (Alloys with Shape Memory Effect) (Translated from Japanese) (Moscow: Metallurgiya, 1990)
9. M Z Mirgazizov, V K Polenichkin, V E Gyunter, V I Itin *Primenenie Splavov s Effektom Pamyati Formy v Stomatologii* (Use of Alloys with the Shape Memory Effect in Stomatology) (Moscow: Meditsina, 1991)
10. V N Zhuravlev, V G Pushin *Splavy s Termomekhanicheskoi Pamyat'yu i ikh Primenenie v Meditsine* (Alloys with Thermomechanical Memory and Their Use in Medicine) (Ekaterinburg: Urals Branch of Russian Academy of Sciences, 2000)
11. H Ludewig *Polyesterfasern* (Berlin: Akademie-Verlag, 1965)
12. K L Gray, in *Chemical Aftertreatment of Textiles* (New York: Wiley, 1971) p. 115
13. W O Statton, in *The Setting of Fibres* (Watford: Merrow, 1971) p. 35
14. A Chiferri, I M Ward (Eds) *Ultra-High Modulus Polymers* (London: Appl. Sci. Publ., 1979)
15. M Trznadel, M Kryszewski *JMS Rev. Macromol. Chem. Phys. C* **32** 259 (1992)
16. M Irie, in *Shape Memory Materials* (Eds K Otsuka, C M Wayman) (Cambridge: Cambridge University Press, 1998) p. 203
17. T Pakula, M Trznadel *Polymer* **26** 1011 (1985)
18. M Trznadel *J. Macromol. Sci. B* **28** 285 (1989)
19. H Kambe, T Kato *Appl. Polym. Symp.* **20** 365 (1973)
20. H Kambe, T Kato, M Kochi *J. Macromol. Sci. A* **8** 157 (1974)
21. Y Tanabe, H Kanetsuna *Polymer* **20** 1121 (1979)
22. M Trznadel, T Pakula, M Kryszewski *Polymer* **26** 1019 (1985)
23. M Trznadel, M Kryszewski *Polymer* **29** 418 (1988)
24. M Trznadel, T Pakula, M Kryszewski *Polymer* **29** 619 (1988)
25. X-Z Yang, J Sun *J. Polym. Sci., Part B* **40** 2646 (2002)
26. N Sun, Z Yuan, J Yang, D Shen *J. Macromol. Sci. B* **39** 397 (2000)
27. N Sun, J Yang, D Shen, R Qian *Chin. J. Polym. Sci.* **18** 69 (2000)
28. X Yang, X Li *Chin. J. Polym. Sci.* **16** 279 (1998)
29. X Yang *Sci. China, Ser. B* **44** 154 (2001)
30. L Lundberg, B Stenberg, J F Jansson *Macromolecules* **29** 6256 (1996)
31. M Doi, S F Edwards, in *The Theory of Polymer Dynamics* (New York: Oxford University Press, 1986)
32. A Lee, R P Wool *Macromolecules* **19** 1063 (1986)
33. D J Brown, A H Windel *J. Mater. Sci.* **19** 1997 (1984)
34. V Skakalova, V Lukes, M Breza *Macromol. Chem. Phys.* **198** 3161 (1997)
35. S S Sheiko, O B Salamatina, S N Rudnev, E F Oleinik *Vysokomol. Soedin., Ser. A* **32** 1844 (1990) [a]
36. E F Oleinik, O B Salamatina, S N Rudnev, S V Shenogin *Vysokomol. Soedin., Ser. A* **35** 1819 (1993) [a]
37. E F Oleinik, O B Salamatina, S N Rudnev, S I Nazarenko, S A Grigoryan *Dokl. Akad. Nauk SSSR* **286** 135 (1986) [b]
38. E F Oleinik *Adv. Polym. Sci.* **80** 49 (1986)
39. J Perez *Physique et Mecanique des Polymers Amorphes* (Paris: Lavoisier, 1992)
40. M B M Mangion, J Y Cavaille, J Perez *Philos. Mag. A* **66** 773 (1992)
41. C Gauthier, J M Pelletier, L David, G Vigier, J Perez *J. Non-Cryst. Solids* **274** 181 (2000)
42. R Quinson, J Perez, M Rink, A Pavan *J. Mater. Sci.* **31** 4387 (1996)
43. R David, R Quinson, C Gauthier, J Perez *Polym. Eng. Sci.* **3** 1633 (1997)
44. T F Oleinik, in *High Performance Polymers* (Eds E Baer, S Moet) (Munich: Hanser-Verlag, 1990) p. 79
45. M S Arzhakov, G M Lukovkin, S A Arzhakov *Dokl. Akad. Nauk* **369** 629 (1999) [b]
46. M S Arzhakov, G M Lukovkin, S A Arzhakov *Dokl. Akad. Nauk* **371** 484 (2000) [b]
47. G M Lukovkin, M S Arzhakov, S A Arzhakov *Dokl. Akad. Nauk* **373** 56 (2000) [b]
48. M S Arzhakov, G M Lukovkin, S A Arzhakov *Dokl. Akad. Nauk* **373** 199 (2000) [b]
49. M S Arzhakov, G M Lukovkin, S A Arzhakov *Dokl. Akad. Nauk* **384** 501 (2002) [b]
50. S A Arzhakov, N F Bakeev, V A Kabanov *Vysokomol. Soedin., Ser. A* **15** 1154 (1973) [a]
51. Yu A Shlyapnokov *Usp. Khim.* **66** 1064 (1997) [*Russ. Chem. Rev.* **66** 963 (1997)]
52. V N Belousov, G V Kozlov, A L Mikitaev, Yu S Lipatov *Dokl. Akad. Nauk SSSR* **313** 630 (1990) [b]
53. A L Volynskii, T E Grokhovskaya, A S Kechek'yan, S L Bazhenov, N F Bakeev *Dokl. Akad. Nauk* **374** 644 (2000) [b]
54. A L Volynskii, A S Kechek'yan, T E Grokhovskaya, V V Lyulevich, S L Bazhenov, A N Ozerin, N F Bakeev *Vysokomol. Soedin., Ser. A* **44** 615 (2002) [a]
55. A L Volynskii, O V Lebedeva, S L Bazhenov, N F Bakeev *Vysokomol. Soedin., Ser. A* **42** 658 (2000) [a]
56. A L Volynskii, T E Grokhovskaya, R Kh Sembaeva, S L Bazhenov, N F Bakeev *Dokl. Akad. Nauk* **363** 500 (1998) [b]
57. A L Volynskii, S L Bazhenov, N F Bakeev *Vysokomol. Soedin., Ser. C* **44** 2352 (2002) [a]
58. A L Volynskii, T E Grokhovskaya, R Kh Sembaeva, I V Yaminskii, L Bazhenov, N F Bakeev *Vysokomol. Soedin., Ser. A* **43** 239 (2001) [a]
59. A L Volynskii, T E Grokhovskaya, R Kh Sembaeva, S L Bazhenov, N F Bakeev *Vysokomol. Soedin., Ser. A* **43** 1008 (2001) [a]

60. A L Volynskii, V N Nechaev, A S Kechek'yan, S L Bazhenov, N F Bakeev *Vysokomol. Soedin., Ser. B* **43** 2211 (2001) [a]
61. A L Volynskii, T E Grokhovskaya, N F Bakeev *Vysokomol. Soedin., Ser. A* **19** 2112 (1977) [a]
62. A L Volynskii, T E Grokhovskaya, A S Kechek'yan, N F Bakeev *Vysokomol. Soedin., Ser. A* **45** 449 (2003) [a]
63. E F Oleinik *Polym. J.* **19** 105 (1987)
64. V A Beloshenko, V N Varyukhin, T P Zaika, S I Skiba, V I Sheludchenko *Fiz. Tekh. Vysok. Davl.* **6** (1) 65 (1996)
65. V A Beloshenko, P V Zamotaev, O P Mityukhin, L M Sergeeva, V F Stroganov *Zh. Prikl. Khim.* **69** 1203 (1996) [c]
66. A A Askadskii, V A Beloshenko, M K Pakter, K A Bychko, M P Valetskii *Vysokomol. Soedin., Ser. A* **33** 2206 (1991) [a]
67. V A Beloshenko, A A Askadskii, V N Varyukhin *Usp. Khim.* **67** 1044 (1998) [*Russ. Chem. Rev.* **67** 951 (1998)]
68. A S Romanov, L S Gladshtein, S I Solomentsev, G V Struminskii *Plast. Massy* (4) 49 (1977)
69. Jpn. P. 56-55 235; *Ref. Zh. Khim.* 9 T 240P (1982)
70. Jpn. P. 57-17 698; *Ref. Zh. Khim.* 15 T 333P (1983)
71. Ukr. P. 10 299; *Promisl. Vlastn.* (4) (1996)
72. Ukr. P. 19 558A; *Promisl. Vlastn.* (6) (1997)
73. Ukr. P. 23 579A; *Promisl. Vlastn.* (4) (1998)
74. Russ. P. 2 141 600; *Byull. Izobret.* (32) (1999)
75. Ukr. P. 29 966A; *Promisl. Vlastn.* (6–11) (2000)
76. Ukr. P. 1332; *Promisl. Vlastn.* (8) (2002)
77. Ukr. P. 10 298; *Promisl. Vlastn.* (4) (1996)
78. Ukr. P. 26 736; *Promisl. Vlastn.* (7) (1999)
79. V A Beloshenko, Ya E Beygelzimer, V F Stroganov, V I Sheludchenko *Eng. Mech.* **7** 231 (2000)
80. V A Beloshenko, A P Borzenko, V F Stroganov, V I Sheludchenko, in *Progressivnye Tekhnologii i Sistemy Mashinostroeniya* (Advanced Processes and Systems in Machine-Building) (Donetsk: Donetsk State Technological University, 2000) p. 49
81. J Bartos, J Muller, J H Wendorff *Polymer* **31** 1678 (1990)
82. G Schoukens, P Samyn, S Maddens, T V Audenaerde *J. Appl. Polym. Sci.* **87** 1462 (2003)
83. J Y Lim, S Y Kim *J. Polym. Sci., Part B* **39** 964 (2001)
84. R G C Arridge, P J Barham, A Keller *J. Polym. Sci., Part B* **15** 389 (1977)
85. A G Gibbson, G R Davies, I M Ward *Polymer* **19** 683 (1978)
86. N B Valiotti, G E Zaikov, V A Timonin, V V Chirikov *Plast. Massy* (11) 35 (1991)
87. O I Chernikov, F S Minevich *Plast. Massy* (11) 59 (1991)
88. P V Zamotaev, S A Sergienko, Z O Strel'tsova *Zh. Prikl. Khim.* **65** 2557 (1992) [c]
89. P V Zamotaev, V A Beloshenko *Zh. Prikl. Khim.* **67** 1863 (1994) [c]
90. V A Beloshenko, G V Kozlov, V G Slobodina, E V Prut, V G Grinev *Vysokomol. Soedin., Ser. B* **37** 1089 (1995) [a]
91. G V Kozlov, V A Beloshenko, V G Slobodina, E V Prut *Vysokomol. Soedin., Ser. B* **38** 1056 (1996) [a]
92. V A Beloshenko, G V Kozlov, V N Varyukhin, V G Slobodina *Acta Polym.* **48** 181 (1997)
93. G V Kozlov, V A Beloshenko, V N Varyukhin, M A Gazaev *Prikl. Mekhan. Tekh. Fiz.* **39** 160 (1998)
94. A G Kozlov, I S Kuryndin, E Yu Rozova, G K El'yashevich *Vysokomol. Soedin., Ser. A* **42** 425 (2000) [a]
95. I S Kuryndin, A V Sidorovich, A M El'yashevich, G K El'yashevich *Vysokomol. Soedin., Ser. B* **44** 1054 (2002) [a]
96. N Tanaka *J. Therm. Anal.* **46** 1021 (1996)
97. P Charoensirisomboon, H Saito, T Inoue, Y Oishi, K Mori *Polymer* **39** 2089 (1998)
98. A Pegoretti, A Guardini, C Migliaresi, T Ricco *Polymer* **41** 1857 (2000)
99. A Pegoretti, A Guardini, C Migliaresi, T Ricco *J. Appl. Polym. Sci.* **78** 1664 (2000)
100. T Ricco, A Pegoretti *J. Polym. Sci., Part B* **40** 236 (2002)
101. W Hu, A Buzin, J-S Lin, B Wunderlich *J. Polym. Sci., Part B* **41** 403 (2003)
102. R J Yan, Y Luo, B Jiang *J. Appl. Polym. Sci.* **47** 789 (1993)
103. P V Zamotaev, E G Privalko, O P Mitukhin, V M Bogdanovich *Ukr. Polym. J.* **1** 221 (1992)
104. V A Bershtein, V M Egorov *Differentsial'naya Skaniruyushchaya Kalorimetriya v Fizikokhimii Polimerov* (Differential Scanning Calorimetry in Physical Chemistry of Polymers) (Leningrad: Khimiya, 1990)
105. O V Kudasheva, E Yu Rozova, E A Karpov, G K El'yashevich *Vysokomol. Soedin., Ser. A* **39** 1635 (1997) [a]
106. G Takakhasi *Plenki iz Polimerov* (Polymer Films) (Translation from Japanese) (Leningrad: Khimiya, 1971)
107. V I Ivanov, A M Bystrov, N N Dyukova *Plast. Massy* (4) 45 (1977)
108. G I Glukhovskaya, A M Kabakchi, V P Gordienko, V V Pokrovskii, V K Ivashchenko, V A Efremov *Plast. Massy* (4) 59 (1977)
109. V I Dakin, V L Karpov *Vysokomol. Soedin., Ser. B* **25** 130 (1983) [a]
110. H Jenkins, A Keller *J. Macromol. Sci. B* **11** 301 (1975)
111. L Mandelkern, R Alomo *Macromolecules* **23** 4721 (1990)
112. A A Kachan, P V Zamotaev *Fotokhimicheskoe Modifitsirovanie Poliolefinov* (Photochemical Modification of Polyolefins) (Kiev: Naukova Dumka, 1990)
113. R Kraus, D Ryan *IEEE Electr. Insul. Mag.* **4** (3) 31 (1988)
114. S Hayashi, N Ishikawa, C Jiordano *J. Coated Fabr.* **23** 74 (1992)
115. H Tobushi, S Hayashi, S Kojima *JSME Int. J. I* **35** 296 (1992)
116. S Hayashi *Int. Prog. Urethanes* **6** 90 (1993)
117. Zh Khou, K Ma, K Zhang, V Zhu, M Syu, K Luo, D Ma *Vysokomol. Soedin., Ser. A* **37** 1377 (1995) [a]
118. T Takahashi, N Hayashi, S Hayashi *J. Appl. Polym. Sci.* **60** 1061 (1996)
119. F K Li, X Zhang, M Xu, X L Luo *Chin. Chem. Lett.* **7** 756 (1996)
120. F Li, X Zhang, J Hou, W Zhu, M Xu *Acta Polym. Sinica* (4) 462 (1996)
121. B K Kim, S Y Lee, M Xu *Polymer* **37** 5781 (1996)
122. F Li, X Zhang, J Hou, M Xu, X Luo, D Ma, B K Kim *J. Appl. Polym. Sci.* **64** 1511 (1997)
123. H M Jeong, B K Kim, Y J Choi *Polymer* **41** 1849 (2000)
124. H M Jeong, S Y Lee, B K Kim *J. Mater. Sci.* **35** 1579 (2000)
125. H M Jeong, J B Lee, S Y Lee, B K Kim *J. Mater. Sci.* **35** 279 (2000)
126. B K Kim, Y J Shin, S M Cho, H M Jeong *J. Polym. Sci., Part B* **38** 2652 (2000)
127. B S Lee, B C Chun, Y C Chung, K I Sul, J W Cho *Macromolecules* **34** 6431 (2001)
128. H Tobushi, K Okumura, S Hayashi, N Ito *Mech. Mater.* **33** 545 (2001)
129. H Tobushi, T Hashimoto, N Ito, S Hayashi, E Yamada *J. Intell. Mater. Syst. Struct.* **9** 127 (1998)
130. H Tobushi, T Hashimoto, S Hayashi, E Yamada *J. Intell. Mater. Syst. Struct.* **8** 711 (1997)
131. H Tobushi, H Hara, E Yamada, S Hayashi *Smart Mater. Struct.* **5** 483 (1996)
132. F Li, J Hou, W Zhu, X Zhang, M Xu, X Luo, D Ma, B K Kim *J. Appl. Polym. Sci.* **62** 631 (1996)
133. B K Kim, S Y Lee, J S Lee, S H Baek, Y J Choi, J O Lee, M Xu *Polymer* **39** 2803 (1998)
134. Y C Lai, E T Quinn, P L Valint *J. Polym. Sci., Part A* **33** 1767 (1995)
135. H M Jeong, B K Ahn, S M Cho, B K Kim *J. Polym. Sci., Part B* **38** 3009 (2000)
136. S Hayashi, S Kondo, P Kapadia, E Ushioda *Plast. Eng.* **51** (2) 29 (1995)
137. US P. 5 957 966 (1999)
138. US P. 6 102 933 (2000)
139. X Luo, X Zhang, M Wang, D Ma, M Xu, F Li *J. Appl. Polym. Sci.* **64** 2433 (1997)
140. H Y Lee, H M Jeong, J S Lee, B K Kim *Polym. J.* **32** 23 (2000)
141. W Tang, W J MacKnight, S L Hsu *Macromolecules* **28** 4284 (1995)
142. A Lendlein, A M Schmidt, R Langer *Proc. Natl. Acad. Sci. USA* **98** 842 (2001)
143. F Li, Y Chen, W Zhu, X Zhang, M Xu *Polymer* **39** 6929 (1998)
144. F K Li, W Zhu, X Zhang, C T Zhao, M Xu *Chin. J. Polym. Sci.* **16** 155 (1998)

145. R D Maksimov, V Kal'kis, T Ivanova, E Plume *Mekhan. Kompozit. Mater.* **38** 305 (2002)
146. R P Kusy, J Q Whitley *Thermochim. Acta* **243** 253 (1994)
147. H M Jeong, J H Song, S Y Lee, B K Kim *J. Mater. Sci.* **36** 5457 (2001)
148. H M Jeong, B K Ahn, B K Kim *Eur. Polym. J.* **37** 2245 (2001)
149. V A Beloshenko, Ya E Beygelzimer, V N Varyukhin *Polymer* **41** 3837 (2000)
150. S Ray Chowdhury, C K Das *J. Appl. Polym. Sci.* **87** 1414 (2003)
151. V A Beloshenko, P V Zamotaev, O P Mityukhin, V G Slobodina *Fiz. Tekh. Vysok. Davl.* **5** (3) 43 (1995).
152. P V Zamotaev, I Khodak, S A Sergienko *Zh. Prikl. Khim.* **66** 2071 (1993) [c]
153. V Kalkis, R D Maksimov, J Zicans *Polym. Eng. Sci.* **39** 1375 (1999)
154. V Kal'kis, R D Maksimov, M Kalnin', Ya Zitsans, T Botsok, O Revyakin *Mekhan. Kompozit. Mater.* **36** 379 (2000)
155. N S Enikolopyan, A M Khachatryan, N M Styrikovich, V G Nikol'skii, A S Kechek'yan *Vysokomol. Soedin., Ser. A* **27** 1685 (1985) [a]
156. M M Dumolin, P J Carreau, L A Utraki *Polym. Eng. Sci.* **27** 1627 (1987)
157. M Levij, F H J Maurer *Polym. Eng. Sci.* **28** 670 (1988)
158. Russ. P. 1 839 148; *Byull. Izobret.* (47 – 48) (1993)
159. R Hill, in *The Mathematical Theory of Plasticity* (Oxford: Clarendon Press, 1998)
160. V Z Aloev, G V Kozlov, I V Dolbin, V A Beloshenko *Izv. KBNTs Ros. Akad. Nauk* (1) 70 (2001)
161. V P Budtov *Fizicheskaya Khimiya Rastvorov Polimerov* (Physical Chemistry of Polymer Solutions) (St Petersburg: Khimiya, 1992)
162. S M Aharoni *Macromolecules* **16** 1722 (1983)
163. G V Kozlov, D S Sanditov *Angarmonicheskie Effekty i Fiziko-Mekhanicheskie Svoistva Polimerov* (Anharmonic Effects and Physical and Mechanical Properties of Polymers) (Novosibirsk: Nauka, 1994)
164. M T Heino, J V Seppala *J. Appl. Polym. Sci.* **48** 1677 (1993)
165. K Engberg, M Ekblad, P-E Werner, U W Gedde *Polym. Eng. Sci.* **34** 1346 (1994)
166. Q Lin, A F Yee *Polymer* **35** 3463 (1994)
167. W Brostow, M Hess, B L Lopez, T Sterzynski *Polymer* **37** 1551 (1996)
168. F P La Mantia, C Geraci, M Vinci, U Pedretti, A Roggero, L I Minkova, P L Magagnini *J. Appl. Polym. Sci.* **58** 911 (1995)
169. R D Maksimov, T Sterzynski, J Garbarczyk *Mekhan. Kompozit. Mater.* **32** 676 (1996)
170. J Zicans, M Kalnins, T Bocoka, V Kalkis, A Bledzki *J. Macromol. Sci. A* **35** 1217 (1998)
171. V Z Aloev, G V Kozlov, V A Beloshenko *Plast. Massy* (8) 11 (2000)
172. V A Beloshenko, A P Borzenko, T P Zaika, E G Pashinskaya *Fiz. Tekh. Vysok. Davl.* **11** (3) 54 (2001)
173. V A Beloshenko, Ya E Beygelzimer, A P Borzenko, V N Varyukhin *Composites A* **33** 1001 (2002)
174. V A Beloshenko, V N Varyukhin, A P Borzenko *High Pres. Res.* **22** 589 (2002)
175. V A Beloshenko, Ya E Beigel'zimer, A P Borzenko, V N Varyukhin, Yu V Voznyak *Vysokomol. Soedin., Ser. A* **45** 597 (2003) [a]
176. V A Beloshenko, Ya E Beigel'zimer, A P Borzenko, V N Varyukhin *Mekhan. Kompoz. Mater.* **39** 379 (2003)
177. F Li, L Qi, J Yang, M Xu, X Luo, D Ma *J. Appl. Polym. Sci.* **75** 68 (2000)
178. N A Kovalenko, I K Syrovatskaya *Plast. Massy* (10) 7 (2000)
179. A Allaoui, S Bai, H M Cheng, J B Bai *Compos. Sci. Technol.* **62** 1993 (2000)
180. N A Kovalenko, I K Syrovatskaya *Plast. Massy* (8) 11 (1999)
181. V E Gul', V P Sokolova, G A Klein, S Z Bondarenko, E A Aripov, A M Berlyand *Plast. Massy* (10) 47 (1972)
182. F Ilmain, T Tanaka, E Kokufuta *Nature (London)* **349** 400 (1991)
183. E S Matsuo, T Tanaka *Nature (London)* **358** 482 (1992)
184. X Zhang, Y Li, Z Xu, C L Littler *J. Chem. Phys.* **102** 551 (1995)
185. Z Xu, X Zhang, Y Li *Science* **269** 525 (1995)
186. Y Osada, A Matsuda *Nature (London)* **376** 219 (1995)
187. Y Osada, S B Ross-Murphy *Sci. Am.* **268** 82 (1993)
188. A Matsuda, J Sato, H Yasunaga, Y Osada *Macromolecules* **27** 7695 (1994)
189. M Irie *Adv. Polym. Sci.* **110** 49 (1993)
190. N Okui, S Umemoto, in *New Functionality Materials* (Eds T Tsuruta, M Doyama, M Seno, Y Imanishi) (Amsterdam: Elsevier, 1993) p. 165
191. Y Osada, J Gong *Prog. Polym. Sci.* **18** 187 (1993)
192. Y Osada, H Okuzaki, H Hori *Nature (London)* **355** 242 (1992)
193. M M Ozmen, O Okay *Eur. Polym. J.* **39** 877 (2003)
194. X-Z Zhang, D-Q Wu, C-C Chu *J. Polym. Sci., Part B* **41** 582 (2003)
195. Y Li, Z Hu, Y Chen *J. Appl. Polym. Sci.* **63** 1173 (1997)
196. X Zhang, Z Hu, Y Li *J. Chem. Phys.* **105** 3794 (1996)
197. S Takata, K Suzuki, T Norisuye, M Shibayama *Polymer* **43** 3101 (2002)
198. T Tanaka *Am. Chem. Soc. Symp.* **480** 1 (1992)
199. Y Li, T Tanaka *Annu. Rev. Mater. Sci.* **22** 243 (1992)
200. M Shibayama, T Tanaka *Adv. Polym. Sci.* **109** 1 (1993)
201. S Hirotsu, Y Hirokawa, T Tanaka *J. Chem. Phys.* **87** 1392 (1987)
202. T Shiga, Y Hirose, A Okada, T Kurauchi *J. Appl. Polym. Sci.* **44** 249 (1992)
203. T Shiga, Y Hirose, A Okada, T Kurauchi *J. Appl. Polym. Sci.* **47** 113 (1993)
204. S A Gordeyev, Yu P Nekrasov *J. Mater. Sci. Lett.* **18** 1691 (1999)
205. A V Rebrov, V A Dubinskii, Yu P Nekrasov, G A Bonartseva, M Shtamm, E M Antipov *Vysokomol. Soedin., Ser. B* **44** 347 (2002) [a]

[a] — *Polym. Sci. (Engl. Transl.)*
[b] — *Dokl. Chem. (Engl. Transl.)*
[c] — *Russ. J. Appl. Chem. (Engl. Transl.)*